MCB
Journals.ASM.org

A *Pitx2*-MicroRNA Pathway Modulates Cell Proliferation in Myoblasts and Skeletal-Muscle Satellite Cells and Promotes Their Commitment to a Myogenic Cell Fate

Estefanía Lozano-Velasco, Daniel Vallejo, Francisco J. Esteban, Chris Doherty, Francisco Hernández-Torres, Diego Franco, Amelia Eva Aránega

Cardiac and Skeletal Myogenesis Group, Department of Experimental Biology, University of Jaén, Jaén, Spain

The acquisition of a proliferating-cell status from a quiescent state as well as the shift between proliferation and differentiation are key developmental steps in skeletal-muscle stem cells (satellite cells) to provide proper muscle regeneration. However, how satellite cell proliferation is regulated is not fully understood. Here, we report that the c-isoform of the transcription factor Pitx2 increases cell proliferation in myoblasts by downregulating microRNA 15b (miR-15b), miR-23b, miR-106b, and miR-503. This *Pitx2c*-microRNA (miRNA) pathway also regulates cell proliferation in early-activated satellite cells, enhancing Myf5$^+$ satellite cells and thereby promoting their commitment to a myogenic cell fate. This study reveals unknown functions of several miRNAs in myoblast and satellite cell behavior and thus may have future applications in regenerative medicine.

The maintenance and repair of adult muscle tissue are directed by satellite cells. Quiescent satellite cells are activated by exercise or injury and enter the cell cycle to produce progeny myogenic precursor cells that undergo multiple rounds of division before entering terminal differentiation and fusing to multinucleated myofibers (1). Together with skeletal muscles, satellite cells originate from cells of the segmented paraxial mesoderm known as somites. Somite formation starts at around embryonic day 7.75 (E7.75) in the mouse embryo and continues until the species-specific number of somites is reached (2). As the somite matures, myogenic progenitor cells become confined to the dorsolateral part of the somite, the dermomyotome. The dermomyotome contains multipotent progenitor cells of different cell types, including the skeletal-muscle progenitors. These cells in the dermomyotome are specified to the myogenic lineage by *Pax3*. Later, *Pax7* is activated within these *Pax3*-expressing myogenic precursors, which produce progenitor cells of the embryonic and fetal body muscles (3, 4). *Pax* genes directly control the activation of the myogenic program in the limb by binding and activating the myogenic regulatory factors Myf5 and Mrf4, followed by MyoD (5–8). *Pax7* is maintained in fetal myogenic precursors and satellite cells in adults, whereas *Pax3* is downregulated during the fetal period (9), although the *Pax3* locus remains active in a subset of satellite cells of particular muscles in adults (10, 11). In adults, satellite cells can be recruited to supply myoblasts for routine muscle fiber homeostasis or for the more sporadic demands of myofiber hypertrophy or repair (12). In addition to producing progeny destined for differentiation, satellite cells also maintain their own population by self-renewal, thus fulfilling the defining criteria of a stem cell (13).

Pitx2, a member of the bicoid family of homeodomain transcription factors, plays a major role in developmental myogenesis. Pitx2 expression occurs in muscle progenitors during musculature development, colabeling with Pax3$^+$ and Pax7$^+$ myotomal cells (14). Moreover, previous works have demonstrated that *Pitx2* can act as an upstream activator of myogenesis in the extraocular muscles, whereas it cooperates with the *Myf5*/*Myf4* pathway to control somite-derived myogenesis (15, 16), and recently, an essential role of Pitx2 and Pitx3 in redox regulation during fetal myogenesis was also reported (17). Previously, we have shown that *Pitx2c* is the main *Pitx2* isoform expressed in Sol8 myoblasts and that overexpression of *Pitx2c* in Sol8 cells displays a high proliferative capacity and completely blocked terminal differentiation of this skeletal-muscle cell line, mainly because high levels of *Pax3* expression were maintained (18). Recent results from our laboratory have revealed that these roles of *Pitx2c* in balancing proliferation versus differentiation as well as signaling through *Pax3* also occur during embryonic myogenesis (19). In addition, the role of Pitx2 during adult myogenesis is beginning to be explored. Recent findings indicate that *Pitx2* is expressed in proliferating satellite cells and can act to promote differentiation of satellite cell-derived myoblasts (20, 21), yet the role of Pitx2 in satellite cell function remains poorly understood. Recent studies have identified the posttranscriptional control mediated by microRNAs (miRNAs) as a crucial level in the regulation of myogenesis. Also, miRNAs have been shown to play crucial roles in muscle development and in the regulation of muscle cell proliferation and differentiation (22, 23). In this context, it has been reported that miRNA 206 (miR-206) and miR-486 induce myoblast differentiation by downregulating *Pax7* (24). More recently, Gagan et al. (25) identified a feed-forward loop where *MyoD* indirectly downregulates its inhibitor

Received 26 May 2015 **Returned for modification** 28 May 2015
Accepted 29 May 2015

Accepted manuscript posted online 8 June 2015

Citation Lozano-Velasco E, Vallejo D, Esteban FJ, Doherty C, Hernández-Torres F, Franco D, Aránega AE. 2015. A *Pitx2*-microRNA pathway modulates cell proliferation in myoblasts and skeletal-muscle satellite cells and promotes their commitment to a myogenic cell fate. Mol Cell Biol 35:2892–2909. doi:10.1128/MCB.00536-15.

Address correspondence to Amelia Eva Aránega, aaranega@ujaen.es.

Supplemental material for this article may be found at http://dx.doi.org/10.1128/MCB.00536-15.

doi:10.1128/MCB.00536-15

TABLE 1 Primers for site-directed mutagenesis[a]

Primer	Sequence
MD15abc_503_1Ccnd1_F	CTCCTCTCATGG*CGC**AAA**TA*CCGATGACTCCCA
MD15abc_503_1Ccnd1_R	TGGGAGTCATCGG*TA**TTT**GCG*CCATGAGAGGAG
MD15abc_503_2Ccnd1_F	TCACGTTGTTTT*CGC**AAA**TA*TTGGAGGGTCAGT
MD15abc_503_2Ccnd1_R	ACTGACCCTCCAA*TA**TTT**GCG*AAAACAACGTGA
MD106ab_Ccnd1_F	ATTCCATTTCAAA*GC**AAA**TT*GGTCAGCTAGCT
MD106ab_Ccnd1_R	AGCTAGCTGACCAA*A**TTT**GC*TTTGAAATGGAAT
MD23abc_Ccnd1_F	TCTATTTTGGCTT*AA**AAA**GA*TTACCGCTGTATT
MD23abc_Ccnd1_R	AATACAGCGGTAA*TC**TTT**TT*AAGCCAAAATAGA
MD15abc_503_1Ccnd2_F	GCTGACTAAAGTAG*C**AAA**TA*CCTAAGGGATATG
MD15abc_503_1Ccnd2_R	CATATCCCTTAGG*TA**TTT**GC*TACTTTAGTCAGC
MD15abc_503_2Ccnd2_F	ATTATTATTTTTC*GC**AAA**TA*AGAAGCTAAGATC
MD15abc_503_2Ccnd2_R	GATCTTAGCTTCT*TA**TTT**GC*GAAAAATAATAAT
MD15abc_503_3Ccnd2_F	TGTTTCACGGTGTG*C**AAA**TA*TTTTAGAAACATT
MD15abc_503_3Ccnd2_R	AATGTTTCTAAAA*TA**TTT**GC*ACACCGTGAAACA
MD106ab_Ccnd2_F	TTCCATTAGAAAAG*C**AAA**TT*GAAAATTTTGGGG
MD106ab_Ccnd2_R	CCCCAAAATTTTC*AA**TTT**GC*TTTTCTAATGGAA
MD106ab_Myf5_F	AATACTGTCTTGCC*A**AAA**TA*TGAGAAAATAGAT
MD106ab_Myf5_R	ATCTATTTTCTCA*TA**TTT**TG*GCAAGACAGTATT

[a] Italics indicate the miRNA seed sequences in the 3′ UTRs of the Ccnd1, Ccdn2, and Myf5 genes. Boldface indicates the directed mutagenesis performed for each seed sequence.

MyoR via miR-378 during myoblast differentiation. In addition, miR-27 has also been implicated in the myogenic process, inducing *in vivo* muscle differentiation and repression of *Pax3* during myogenic differentiation (26). We have recently shown that *Pitx2c* plays an important role during myogenic development, controlling miR-27 and *Pax3* expression and thus maintaining the cells in a predifferentiated state. Furthermore, miRNAs modulate stem cell fate decisions, and some miRNAs involved in satellite cell quiescence and activation are starting to be identified (27–29). In the present study, we have further elaborated the transcriptional regulation of miRNAs by *Pitx2* in myoblasts and satellite cells, aiming to unravel whether impaired microRNA expression mediated by *Pitx2* might contribute to the cellular and molecular phenotypes previously reported, i.e., increased cell proliferation.

MATERIALS AND METHODS

Microarrays and statistical and bioinformatics analyses. In the present study, mirVana microarrays (Ambion) were used to profile the microRNA signature under different *Pitx2c* overexpression conditions, namely, two different doses (400 and 800 ng/ml of the cytomegalovirus [CMV]-Pitx2c plasmid) after 24 h of transfection. Thirty micrograms of total RNA was used to hybridize the distinct microRNA microarrays under each condition analyzed. MicroRNA-Cy5 labeling, microarray hybridization, and washing steps were performed according to the manufacturer's guidelines. The obtained original raw data files included quadruplicates of any given microRNA probe (662 unique mouse/human/rat mature microRNAs). Thus, the raw intensity value for each replicate of the same probe was considered an independent sample under each condition and then normalized by using the "justvsn" function implemented in the "vsn" Bioconductor library (http://bioconductor.org/) run in R software (http://r-project.org/). The normalized data were then uploaded and analyzed with the TM4 microarray software suite (http://tm4.org/), where a one-way analysis of variance (ANOVA) was carried out; those microRNAs showing a false-significant proportion of <0.05 were selected as significant, and their expression levels were used to obtain gene hierarchical clustering (using Pearson absolute correlation and complete-linkage algorithms).

DNA plasmid/siRNA transfection experiments and luciferase assays. DNA plasmid and small interfering RNA (siRNA) transfections were performed in Sol8 myoblasts, as previously described (19). The DNA plasmids used were the CMV-Pitx2c and CMV-enhanced green fluorescent protein (EGFP) plasmids. For RNA interference, siRNA against Pitx2c (Sigma) was used (19). For luciferase assays, the *cyclin D1*, *cyclin D2*, and *Myf5* 3′ untranslated regions (UTRs) were amplified from mouse genomic DNA and cloned into the pGLuc-Basic vector (New England BioLabs). Cyclin D1, cyclin D2, and Myf5 gene 3′ UTRs were amplified from mouse genomic DNA with specific primers bearing HindIII/BamHI restriction sites and cloned into the pGLuc-Basic vector (New England BioLabs). PCR-based site-directed mutagenesis was performed by using the Stratagene QuikChange site-directed mutagenesis kit but with the enzymes and buffers from the Bio-Rad iPROOF PCR kit. Primers used for site-directed mutagenesis (Table 1) introduced mutations into miR-15b, miR-106b, miR-23b, and miR-503 seed sequences present in the *cyclin D1* 3′ UTR, *cyclin D2* 3′ UTR, and *Myf5* 3′ UTR. Independent cotransfection experiments with pre-miRNAs were carried out simultaneously in Sol8 cells with 20 μl of culture medium; luciferase activity was measured 24 h after transfection by using a BioLux Gaussia luciferase assay kit or a BioLux Cypridina luciferase assay kit (New England BioLabs). In all cases, transfections were carried out in triplicate.

Generation of conditional tissue-specific null mutant mice. *Pax3*-Cre transgenic mice, purchased from the Jackson Laboratory, were crossed into homozygous *Pitx2* floxed mice, and *Pax3-cre*$^{+/-}$ *Pitx2*$^{fl+/-}$ heterozygotes were backcrossed. The littermates were PCR screened with *Pitx2*- and Cre-specific primers (30). Cre-positive heterozygote mice were selected as wild-type controls (*Pax3-cre*$^{+/-}$). All mice were maintained inside a barrier facility, and experiments were performed in accordance with University of Jaén regulations for animal care and handling.

Satellite cell isolation. Satellite cells were isolated as described previously by Qu-Petersen et al. (31). Two populations of early-preplate (EP) cells were used: EP cells after 3 days of culturing, which were previously described as phenotypically EPq, relatively quiescent early-activated cells, and EP cells after 5 days of culturing, which were previously described as phenotypically EPa, activated cells (31). Primary muscle cultures were prepared from young (3- to 4-month-old) normal mice by using a modified version of a previously described preplate technique (32–36). The hind limb muscles of young mice were removed, and the bones were dissected. The muscle was then minced into a coarse slurry by using scalpels. The muscle tissue was enzymatically dissociated at 37°C in 0.2% collagenase type XI (Sigma-Aldrich) for 1 h and then centrifuged at 3,500 rpm for 5 min. The cells were collected, incubated in dispase (Gibco BRL), prepared as 2.4 U/1 ml Hanks balanced salt solution (HBSS) (Gibco BRL)

TABLE 2 Specific primers for each gene, annealing temperatures, and amplicon sizes

Gene	Direction	Primer	Annealing temp (°C)	Amplicon size (bp)
β-*actin*	Sense	5′-CCA GAG GCA TAC AGG GAC-3′	60	143
	Antisense	5′-TGA GGA GCA CCC TGT GCT-3′		
Gapdh	Sense	5′-TCT TGC TCA GTG TCC TTG CTG G-3′	60	180
	Antisense	5′- TCC TGG TAT GAC AAT GAA TAC GC-3′		
Pitx2c	Sense	5′-CCT CAC CCT TCT GTC ACC AT-3′	60	175
	Antisense	5′-GCC CAC ATC CTC ATT CTT TC-3		
ccnd1	Sense	5′-TTG ACT GCC GAG AAG TTG TG-3′	60	154
	Antisense	5′-CTG GCA TTT TGG AGA GGA AG-3′		
ccnd2	Sense	5′-ATG CTG CTC TTG ACG GAA CT-3′	60	201
	Antisense	5′-ATG CTG CTC TTG ACG GAA CT-3′		
Pax7	Sense	5′-ACC ACT TGG CTA GGA TTT TCA AG-3′	60	240
	Antisense	5′- AGT AGG CTT GTC CCG TTT CC-3′		
Myf5	Sense	5′-TGA GGG AAC AGG TGG AGA AC-3′	60	187
	Antisense	5′-AGC TGG ACA CGG AGC TTT TA-3′		

TABLE 3 Specific primers for each miRNA analyzed

MicroRNA	Primer
hsa-miR-1	UGGAAUGUAAAGAAGUAUGUAU
hsa-miR-15a	UAGCAGCACAUAAUGGUUUGUG
hsa-miR-15b	UAGCAGCACAUCAUGGUUUACA
hsa-miR-21	UAGCUUAUCAGACUGAUGUUGA
hsa-miR-23a	AUCACAUUGCCAGGGAUUUCC
hsa-miR-23b	AUCACAUUGCCAGGGAUUACC
hsa-miR-106b	UAAAGUGCUGACAGUGCAGAU
hsa-miR-130a	CAGUGCAAUGUUAAAAGGGCAU
hsa-miR-133a	UUUGGUCCCCUUCAACCAGCUG
hsa-miR-206	UGGAAUGUAAGGAAGUGUGUGG
hsa-miR-503	UAGCAGCGGGAACAGUUCUGCAG

for 45 min, and then incubated for 30 min in 0.1% trypsin-EDTA (Gibco BRL) diluted in HBSS. After enzymatic dissociation, the muscle cells were centrifuged and resuspended in proliferation medium (PM). PM consists of Dulbecco's modified Eagle's medium containing 10% horse serum, 10% fetal bovine serum (FBS), 0.5% chicken embryo extract, and 1% penicillin-streptomycin (all reagents were purchased from Gibco BRL). Different populations of muscle-derived cells were isolated based on their adhesion characteristics. The muscle cells were plated into collagen-coated flasks (collagen type I; Sigma-Aldrich) for 2 h (preplate 1 [pp1]). The nonadherent cells were then transferred to other flasks (pp2), and the adherent cells in pp1 were discarded. It has been reported that the cells that rapidly attach are highly fibroblastic in nature (32–35). After 24 h, the floating cells in pp2 were collected, centrifuged, and plated into new flasks (pp3). These procedures were repeated at 24-h intervals until serial preplates (pp5) were obtained. All cell populations (pp3 to pp5) were maintained in PM with daily changes. Based on data from a previous report (31), 30 to 40% of the cells in pp2 and pp3 are known to be nonmyogenic, whereas up to 95% desmin-negative cells can be found in pp4 and pp5 (35). To further purify the myogenic cell population, pp2 and pp3 were discarded, and only pp4 and pp5 were combined and termed the EP cell population, as previously described (36).

Lentiviral vector production and satellite cell transduction. For the construction of the *Pitx2c* expression cassettes, the coding region of mouse *Pitx2c* was PCR amplified and cloned into pGEM-T. After sequence verification, the DNA was subcloned into the lentiviral vector pLVX-IRES-ZsGreen1 (Clontech), which allows the simultaneous expression of Pitx2c protein and a green fluorescent protein (ZsGreen1) and sequencing for verification. The recombinant DNA was cotransfected with a mixture of plasmids that express the respective viral proteins needed for producing viral particles in packing cells (Lenti-X 293T), by using Lenti-X HTX packaging systems according to the manufacturer's instructions (Clontech). The titer of lentivirus was determined by transducing Lenti-X 293T cells and by using the Lenti-X reverse transcriptase quantitative PCR (qRT-PCR) titration kit (Clontech). Freshly isolated satellite cells (EPq and EPa) were transduced with lentiviral vectors coding for Pitx2c (pLVX-Pitx2c-ZsGreen) or empty lentiviral vector cDNA (pLVX-IRES-ZsGreen1), at a multiplicity of 50 to 100 genome units, determined by quantitative PCR (qPCR), and adsorption of the lentiviral vectors was done for 8 to 24 h on cultures after viral particles were added. Transduction was monitored in all experiments by flow cytometry and by fluorescence microscopy.

Flow cytometry and fluorescence microscopy. Cells were fixed with 4% paraformaldehyde. ZsGreen1-positive (ZsGreen1$^+$) cells were analyzed by flow cytometry using an LSR-Fortessa cytometer (Beckman Coulter, Brea, CA). DNA was stained with 4′,6-diamidino-2-phenylindole (DAPI; Sigma-Aldrich). Fluorescence microscope images were acquired with a Leica TCS SL confocal microscope (Leica LCS version 2.0).

MicroRNA and anti-microRNA transfection assays. Sol8 cells as well as EPq and EPa satellite cells were cultured under growth conditions. The corresponding pre-miRNAs (Ambion) were transfected as described previously (19).

qRT-PCR analyses. RNA isolation and RT-PCR were performed as described previously (19), using standard procedures. Total RNA was extracted from mouse muscle tissue, Sol8 cells, EPq cells, EPa cells, and differentiating myoblasts by using the TriPure isolation reagent (Roche) according to the supplier's guidelines. To minimize genomic DNA contamination, total RNA was treated with 20 U of RNase-free DNase (Roche) for 1 h at 37°C and then purified by using a standard phenol-chloroform protocol. One microgram of total RNA was reverse transcribed by using Superscript RNase H$^-$ reverse transcriptase (Invitrogen) or an Exiqon microRNA qRT-PCR detection system, according to the manufacturer's protocol. As a reverse transcription control, each sample was subjected to the same process without reverse transcriptase. Real-time PCR was performed by using an MxPro Mx3005p PCR thermal cycler (Stratagene, Spain) and a SYBR green detection system (DyNamo HS SYBR green qPCR kit; Finnzymes). PCRs were performed in 0.2-ml optical tubes (Cultek) with a 20-μl total volume containing SYBR green mix (Finnzymes) and 2 μl of the reverse-transcribed RNA. The β-*actin* and *Gapdh* genes were used in parallel for each run as an internal control. Amplification conditions were 95°C for 5 min and 40 cycles of 95°C for 30 s, the annealing temperature for 30 s, and 72°C for 30 s. The final cycle was performed at 72°C for 7 min. Specific primers for each gene analyzed, annealing temperatures, and amplicon sizes are shown in Table 2. The

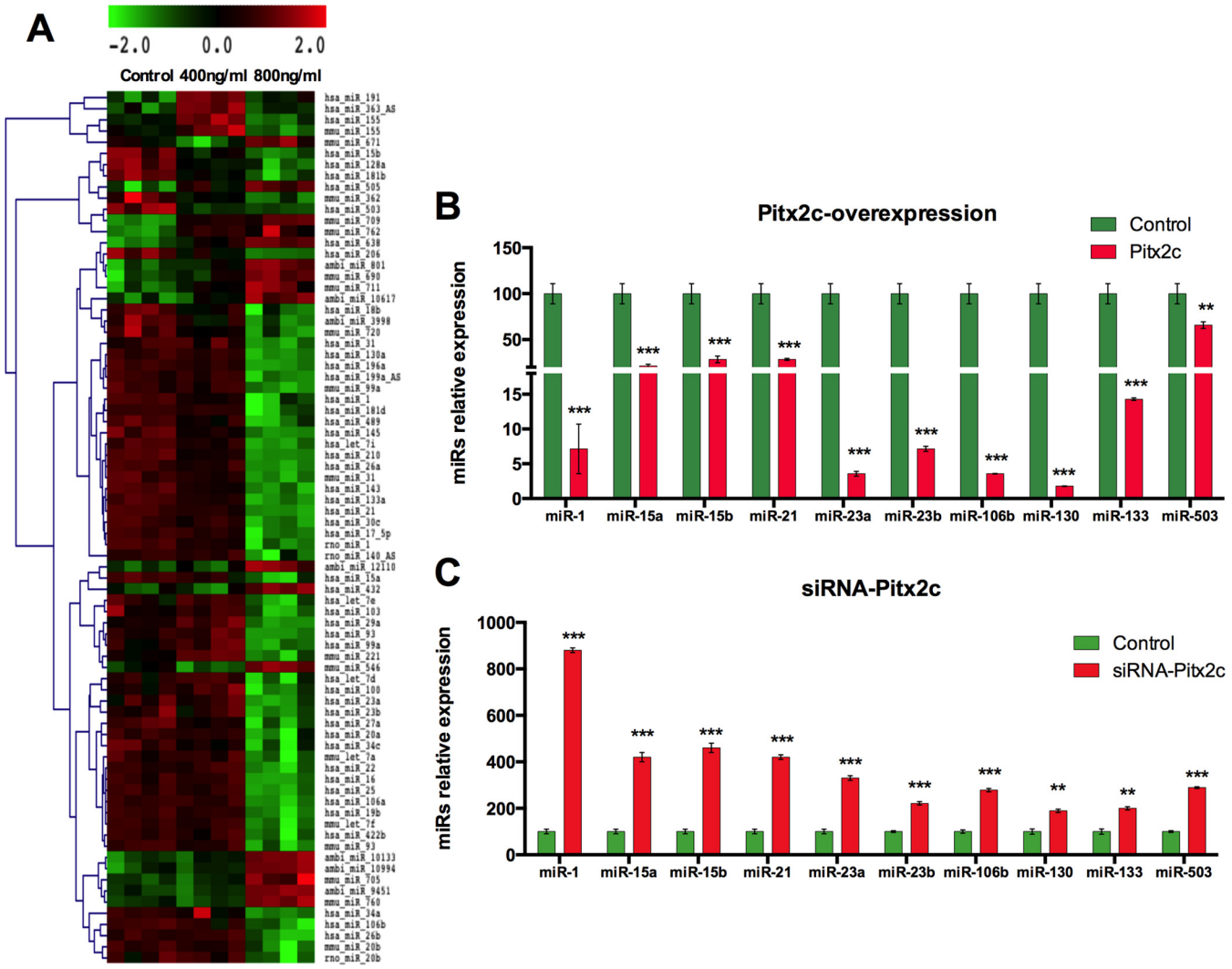

FIG 1 (A) Hierarchical clustering of statistically significant microRNA microarray expression profiles with the Sol8 cell line transfected with 400 ng/ml and 800 ng/ml of the CMV-*Pitx2c* plasmid 24 h after transfection. The color range (−2 to 2) is related to Z-scored expression values. (B) Expression profiles of statistically significant miRNAs by qRT-PCR in Sol8 *Pitx2c*-transfected cells at 400 and 800 ng/ml of the Pitx2c plasmid compared to controls. (C) Expression profiles of the statistically significant miRNAs by qRT-PCR in *Pitx2c*-silenced Sol8 cells (siRNA against Pitx2c) compared to controls.

relative level of expression of each gene was calculated as the ratio of the extrapolated levels of expression of each gene to the *Gapdh* level. PCR product sizes were verified by 2% agarose gel electrophoresis. For each pool of cDNA used, Pitx2c expression was confirmed. Each PCR was performed in triplicate and repeated with at least three different biological samples to obtain a representative average.

For microRNAs, qRT-PCRs were performed by using the Exiqon LNA microRNA primers and detection kit according to the manufacturer's guidelines. All reactions were always run in triplicates by using 5S as a normalizing control, as recommended by the manufacturer. SYBR green was used as a quantification system on a Stratagene Q-Max 2005P qRT-PCR thermocycler. Relative measurements were calculated as described previously by Livak and Schmittgen (37), and control measurements were normalized to represent 100%, as previously described (38). Specific primers for each miRNA analyzed are shown in Table 3.

***In situ* hybridization.** *In situ* hybridization was performed on serial cryosections of limb muscles obtained from C57BL/10 mice by using double-digoxigenin (DIG)-labeled LNA oligonucleotides (Exiqon) or antisense RNA probes, as previously described (39). Combined immunohistochemical detection was performed as previously described (40), by using anti-Pax7 antibody (Developmental Hybridoma Bank).

Immunocytochemistry. Immunocytochemistry experiments with Sol8 cell cultures and EPq and EPa cultured satellite cells were performed as described previously (14, 19). The antibodies used for immunostaining included anti-Ki67 (Abcam) anti-Myf5 (Santa Cruz Biotechnology), and anti-PHH3 (Millipore). For immunofluorescence, fluorochrome (Alexa Fluor 546)-conjugated secondary anti-rabbit antibodies (Invitrogen) were used for visualization. Nuclear staining was performed by using DRAQ-5 (red fluorescent cell-permeable DNA probe; Biostatus Limited). Immunofluorescence detection was performed by confocal analyses using a Leica TCS SL confocal microscope (Leica LCS version 2.0). Quantification was performed at a ×10 magnification for PHH3-positive cells and at a ×20 magnification for Ki67- and Myf5-positive cells; each experimental point is represented by the average of data from analyses of five different images for each independent experiment, and experiments were repeated with at least three different biological samples to obtain a representative average.

Chromatin immunoprecipitation assays. Chromatin immunoprecipitation (ChIP) assays were performed as described previously (41),

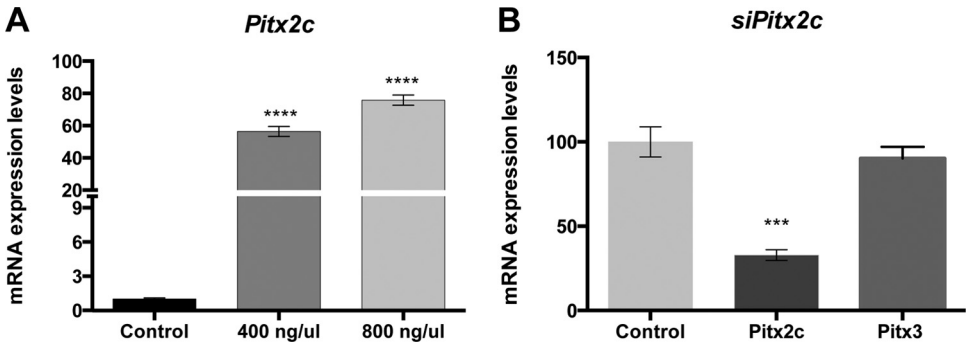

FIG 2 (A) qRT-PCR analyses showing *Pitx2c* overexpression after transfection with two different doses of the CMV-*Pitx2c* plasmid (400 and 800 ng/ml). (B) mRNA expression levels of Pitx2c and Pitx3 after treatment with siRNA against *Pitx2* in Sol8 myoblasts.

with modifications. Sol8 cells were transfected with 8 μg of the pcDNA-V5-Pitx2c plasmid in 100-mm dishes. After 24 h of Pitx2c transfection, the cells were cross-linked with 1% formaldehyde for 10 min at 37°C. For chromatin immunoprecipitation, the antibodies used were anti-V5 (clone V5-10; Sigma) or anti-polymerase II (anti-Pol II) (8WG16) (Santa Cruz); antibody against mouse dystrophin was used as a mouse IgG control. All PCRs were performed at an annealing temperature of 60°C. Different primers were used to amplify the DNA regions containing the Pitx2 binding site 6 kb upstream of the coding sequences for miR-15b, miR-106b, miR-503, and miR-23b (Table 3). As controls, normal rabbit IgG replaced the anti-V5 antibody to reveal nonspecific immunoprecipitation of chromatin. Three parallel real-time PCRs were also performed in triplicate with dilutions of input DNA to determine the linear range of amplification. Enrichment of RNA polymerase II served as an internal positive control for the ChIP assays, which was observed in all DNA regions analyzed.

Statistics. Data are presented as means, with error bars representing standard deviations. Data were analyzed for significance by Student's *t* test and considered significantly different if the *P* value was <0.01.

Microarray data accession number. The data discussed here have been deposited in the NCBI Gene Expression Omnibus (GEO) (42) and are accessible through GEO series accession number GSE53943 (http://www.ncbi.nlm.nih.gov/geo/query/acc.cgi?acc=GSE53943).

RESULTS

Pitx2-mediated microRNA expression in skeletal myoblasts. Pitx2 is expressed in developing myoblasts very early in development, and it was recently demonstrated to play a pivotal role in regulating key myogenic steps. We previously documented that *Pitx2c* is key in modulating proliferation versus differentiation and balancing different progenitor cell populations during myo-

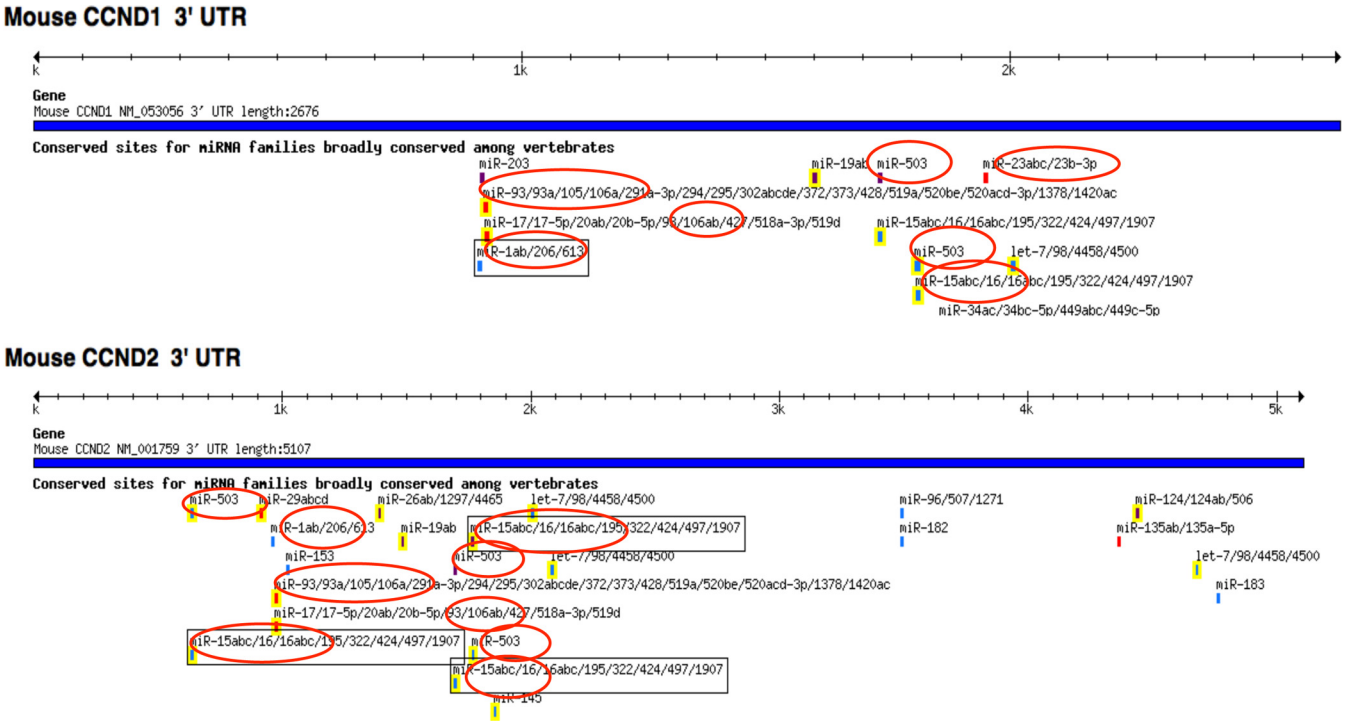

FIG 3 Schematic representation of the putative microRNA binding sites in the cyclin D1 (*ccnd1*) and cyclin D2 (*ccnd2*) genes as revealed by the TargetScan algorithm (http://www.targetscan.org/).

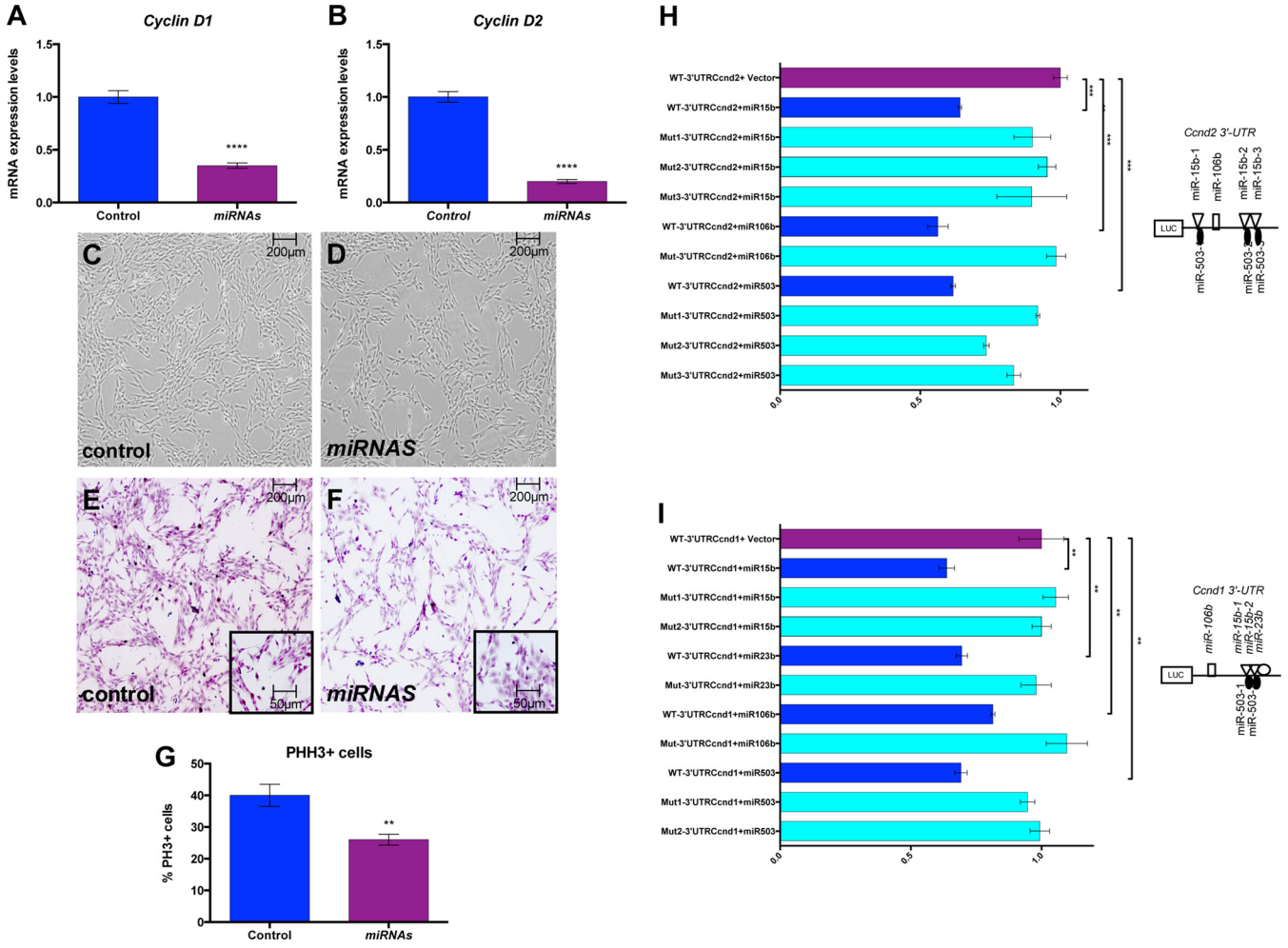

FIG 4 (A and B) Expression levels of *ccnd1* and *ccnd2* in Sol8 cells overexpressing a cocktail of miR-15b, miR-23b, miR-106b, and miR-503 (miRNAs) compared to control cells. (C and D) Representative images of Sol8 cells transfected with the miRNA cocktail and control cell cultures. (E and F) Representative images of immunohistochemical PHH3 staining in the Sol8 cell line overexpressing miRNA compared to controls. The inset represents closeup views of the corresponding immunostained cells. (G) Quantification of $PHH3^{+}$/total cells in transfected Sol8 cells compared to controls after 24 h of miRNA transfection. (H and I) Normalized luciferase activity of the 3′-UTR cyclin D1 and cyclin D2 gene luciferase reporter (wild type [WT] *cyclin D1* and wild-type *cyclin D2* 3′ UTRs) with an empty plasmid or pre-miRNAs shows a loss of luciferase activity with expression of miR-15b, miR-23b, miR-106b, and miR-503. There was no loss of luciferase activity when the miRNA seed sequences were mutated.

genesis. Furthermore, we have shown that *Pitx2c* posttranscriptionally modulates key myogenic transcription factors such as Pax3 by repressing miR-27 expression (18, 19). To further analyze the role of *Pitx2c* in the posttranscriptional control of myogenesis, we performed microRNA microarray analyses using *Pitx2c*-overexpressing Sol8 myoblasts. Because we previously demonstrated that *Pitx2c*-mediated effects on myoblasts are dose dependent, we used two different doses of the CMV-*Pitx2c* plasmid (400 and 800 ng/ml of the CMV-*Pitx2c* plasmid), which previously affected myoblast proliferation and differentiation (19), thereby providing insights into the dose dependency of *Pitx2*-regulated miRNAs (http://www.ncbi.nlm.nih.gov/geo/query/acc.cgi?acc=GSE53943). Figure 1A illustrates the hierarchical clustering of differentially expressed and statistically significant miRNAs after 24 h of cell transfection. Of 497 miRNAs, 60 (~10%) displayed statistically significant differences, thus suggesting that they are regulated by *Pitx2*. Detailed analyses demonstrated at least four distinct expression patterns. Small proportions of miRNAs display higher levels (7/60; ~11%) or lower levels in transfections with both doses of the CMV-*Pitx2c* plasmid (Fig. 1A). Most miRNAs (40/60; ~67%) display significantly lower expression levels only at *Pitx2c* doses previously shown to have more profound effects on the myoblast phenotype (transfections with 800 ng/ml of the CMV-*Pitx2c* plasmid) (Fig. 1A), while only a minority (1/60; ~1%) showed increased expression levels at this dosage. The remaining miRNAs displayed a transient increase (2/60; ~3%) or decrease (3/60; ~5%) of expression levels at low doses (transfections with 400 ng/ml of the CMV-*Pitx2c* plasmid). Overall, these data illustrate that *Pitx2* regulates the expression of different subsets of miRNAs. Importantly, most miRNAs regulated by *Pitx2* in skeletal-muscle myoblasts displayed lower levels (50/60; ~83%), and only a small proportion (10/60; ~17%) showed higher expression levels. We validated our microarray expression data by using qRT-PCR. As illustrated in Fig. 1B and 2A, miR-1, miR-15a, miR-15b, miR-21, miR-23a, miR-23b, miR-106b, miR-130, miR-133, and miR-503 displayed significantly lower levels after *Pitx2c* overexpression,

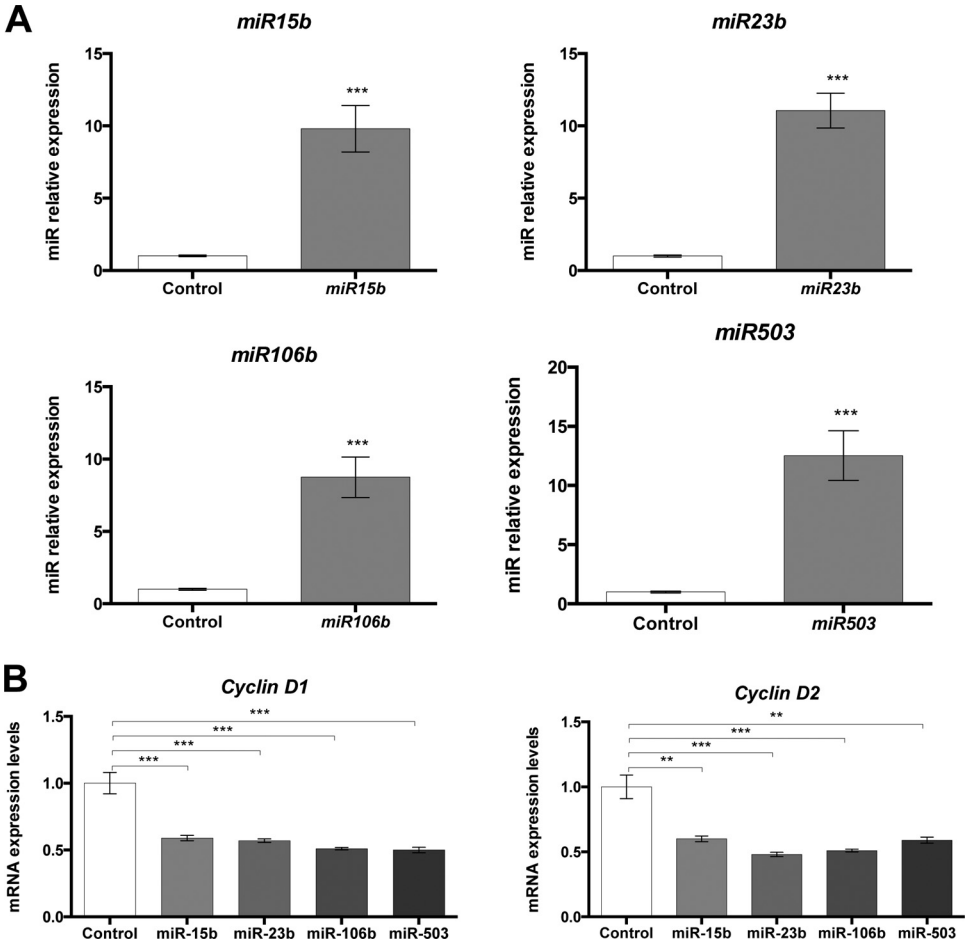

FIG 5 (A) qRT-PCR analyses showing miRNA overexpression after pre-miRNA-independent transfections. (B) mRNA expression levels for cyclin D1 and cyclin D2 genes were 50 to 60% lower when miRNAs were transfected separately in Sol8 cells.

whereas siRNA against *Pitx2* in Sol8 myoblasts resulted in the upregulation of miR-1, miR-15a, miR-15b, miR-21, miR-23a, miR-23b, miR-106b, miR-130, miR-133, and miR-503 (Fig. 1C and 2B), supporting our microarray observations. Individual miRNAs can target a large number of transcripts, and thus, their functional roles can vary greatly according to the biological context. To provide an initial insight into the putative mechanisms by which *Pitx2*-regulated miRNAs can exert their function in skeletal-muscle myoblasts, we undertook gene ontology analyses using DAVID software (http://david.abcc.ncifcrf.gov/). These gene ontology analyses revealed that the *Pitx2*-upregulated and *Pitx2*-downregulated miRNAs might modulate highly similar pathways: transcription, regulation of transcription, cell morphogenesis, and cell proliferation (see Table S1 in the supplemental material). In addition, cell projection, cell organization, cell motility, cell proliferation, and cell maturation were also revealed for *Pitx2*-downregulated miRNAs (see Table S1 in the supplemental material). Overall, these data support the notion that cell behavior and proliferation pathways induced by *Pitx2* could be driven by microRNA expression in myoblasts.

Role for *Pitx2*-mediated microRNAs in regulating myoblast cell proliferation. Previously, we demonstrated that overexpression of *Pitx2c* in mouse myoblasts leads to greater cell proliferation and loss of the ability to fuse and thus to form myotubes and terminally differentiate (18). *Pitx2* overexpression raises levels of *Pax3* expression, which in turn inhibits *MyoD* and myogenin gene expression and terminal differentiation, a process mediated by *Pitx2* regulation of miR-27 (19). However, cell proliferation in *Pitx2c*-overexpressing myoblasts is independent of *Pax3* and/or miR-27 regulation (19). Additionally, a role of Pitx2 in controlling myocyte numbers on the chick myotome has been reported (43), suggesting that the effect of Pitx2 on cell proliferation in myogenic cells is conserved in different vertebrate species. Thus, we focused our attention on whether deregulation of other miRNAs, mediated by Pitx2, can affect cell cycle regulation. We bioinformatically analyzed the putative microRNAs targeting key genes of cell cycle regulation, such as the cyclin D1 (*ccnd1*) and cyclin D2 (*ccnd2*) genes, and we found that >65% of the predicted target sites for microRNA in the *ccnd1* (8/12) and *ccnd2* (11/16) 3′ UTRs correspond to four downregulated miRNAs in Sol8 after *Pitx2c* overexpression (Fig. 3). Thus, these data suggest that Pitx2 controls transcriptional inhibition of a large subset of miRNAs, which in turn can modulate cell proliferation in Sol8 myoblasts. Notably, except for miR-1 and miR-206 (22), the role of these miRNAs in the regulation of cell proliferation on skeletal-muscle cells has not been reported previously. To investigate the function of miRNAs regulated by Pitx2 with previously unknown functions in myoblast cell proliferation, such as miR-15b, miR-23b, miR-106b, and

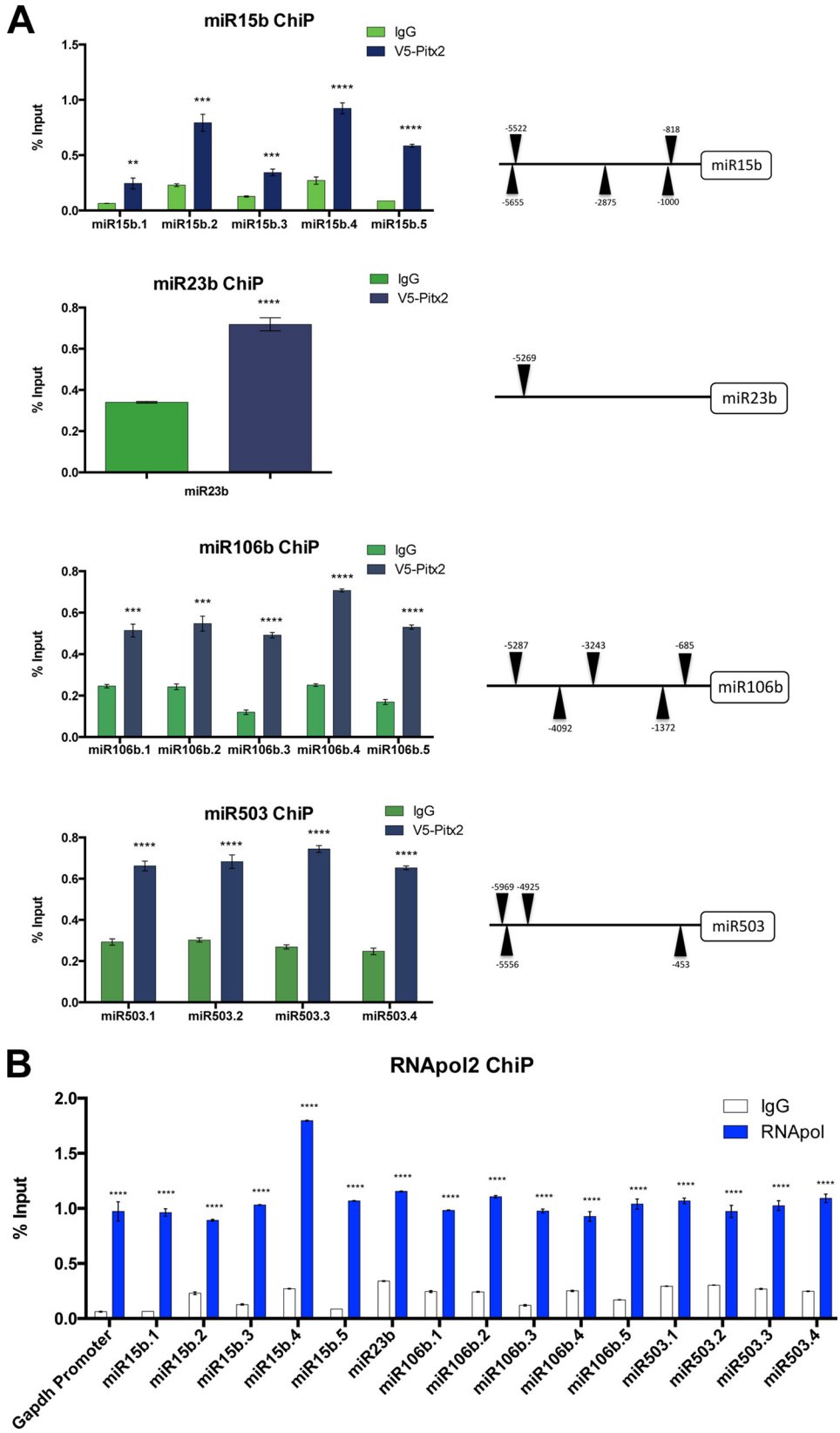

FIG 6 (A) ChIP assays. Pitx2 binds DNA regions upstream of the miR-15b, miR-23b, miR-106b, and miR-503 genetic loci. There was an observed enrichment in Pitx2 binding in all miRNAs analyzed. ***, $P < 0.001$; **, $P < 0.01$; *, $P < 0.05$. These experiments were performed in Sol8 cells. (B) RNA polymerase II occupancy in the tested DNA regions upstream of miR-15b, miR-23b, miR-106b, and miR-503. Notably, all of these DNA regions have RNA polymerase II occupancy levels similar to those of the *Gapdh* promoter used as a control.

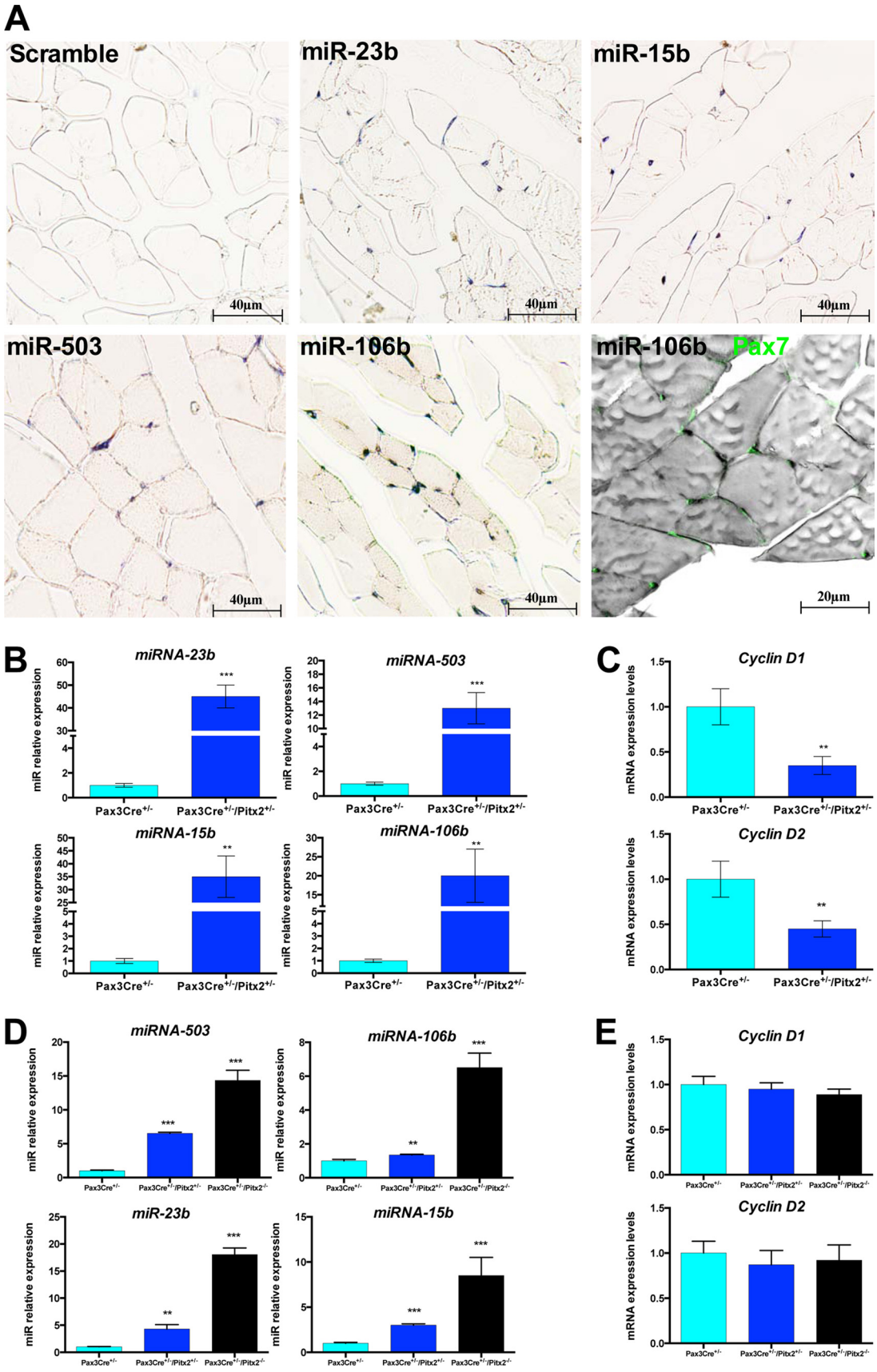

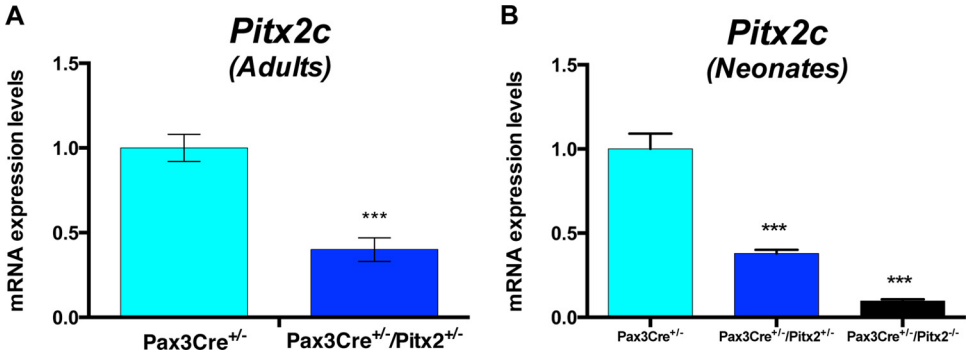

FIG 8 (A) qRT-PCR for *Pitx2c* expression in *Pax3-cre*$^{+/-}$/*Pitx2*$^{+/-}$ heterozygote adult mice. (B) qRT-PCR for *Pitx2c* expression in *Pax3-cre*$^{+/-}$/*Pitx2*$^{+/-}$ heterozygote and *Pax3-cre*$^{+/-}$/*Pitx2*$^{-/-}$ homozygote neonates.

miR-503, we performed transfection experiments with these miRNAs on Sol8 myoblasts at low confluence (10^5 myoblasts/well) and assessed cell proliferation by phospho-histone 3 immunolabeling after 24 h of transfection. In addition, cyclin D1 and cyclin D2 gene expression levels were measured by qRT-PCR. As reflected in Fig. 4A and B, transfection experiments with a cocktail of these miRNAs resulted in 80% lower expression levels of the cyclin D1 and cyclin D2 genes. In line with these findings, cells displayed a lower phospho-histone 3-immunolabeled index and thus were clearly proliferating at a slower pace, as illustrated in Fig. 4C to G. To test whether the predicted miR-15b, miR-23b, miR-106b, and miR-503 elements in the 3′ UTRs of the cyclin D1 and cyclin D2 genes were functional, we ligated these sequences downstream of the luciferase gene in the pGLuc-Basic vector and cotransfected them independently with pre-miR-15b, pre-miR-23b, pre-miR-106b, and pre-miR-503 into Sol8 cells (Fig. 4H and I). Luciferase activity for the cyclin D1 and cyclin D2 gene 3′ UTRs was approximately halved with cotransfection with pre-miR-15b, pre-miR-23b, pre-miR-106b, and pre-miR-503 compared with the empty vector, and importantly, site-directed mutagenesis of the predicted pre-miR-15b, pre-miR-23b, pre-miR-106b, and pre-miR-503 binding sites in the cyclin D1 and cyclin D2 gene 3′ UTRs eliminated such repression (Fig. 4H and I). Transfection with pre-miR-15b, pre-miR-23b, pre-miR-106b, and pre-miR-503a separately decreased the expression levels of the cyclin D1 and cyclin D2 genes only 50 to 60% (Fig. 5), suggesting synergism or additive effects among them.

In order to reinforce the notion that Pitx2 directly modulates the expression of these four miRNAs, we screened for potential conserved *Pitx2* binding sites upstream of the miR-15b, miR-23b, miR-106b, and miR-503 genetic loci. Five conserved Pitx2 binding sites were identified ~6 kb upstream of the miR-15b and miR-106b genetic loci, four sites were identified ~6 kb upstream of the miR-503 genetic locus, and one site was located ~6 kb upstream of the miR-23b gene locus (Fig. 6A). To test the interaction of Pitx2 with these putative binding sites, we performed chromatin immunoprecipitation (ChIP) assays in Sol8 cells. Exogenous Pitx2 bound to the all-putative binding sites upstream of the miR-15b, miR-23b, miR-106b, and miR-503 genetic loci, as illustrated in Fig. 6A. RNA polymerase II occupancy suggests that all DNA regions tested are transcriptionally active (Fig. 6B). Taken together, these data point out a *Pitx2*-miRNA pathway controlling the expression of key regulatory cell cycle genes, which in turn modulate cell proliferation in myoblasts.

***Pitx2*-mediated miRNAs and regulatory cell cycle gene expression are deregulated in conditional tissue-specific *Pitx2* mutant mice.** First, we checked the expression pattern for miRNAs regulated by *Pitx2c* in serial sections obtained from wild-type mouse limb muscles by LNA *in situ* hybridization. As illustrated in Fig. 7A, miR-15b, miR-23b, miR-106b, and miR-503 displayed a tissue expression pattern compatible with marked expression on satellite cells. Second, to determine whether *Pitx2c*-mediated miRNA regulation on myogenic cells is maintained *in vivo*, we used qRT-PCR to analyze the expression levels of miRNA regulated by *Pitx2c* in conditional tissue-specific *Pitx2* mutant mice by intercrossing a *Pitx2* floxed mouse line with a *Cre* deleter mouse line, which rendered muscle lineage-specific *Pax3-Cre* recombination. This conditional mutant mouse line is currently being analyzed and characterized (E. Lozano-Velasco, F. Ramirez, P. Hernández-Torres, D. Vallejo, D. Franco, and A. E. Aránega, unpublished data). Because *Pax3-cre*$^{+/-}$/*Pitx2*$^{-/-}$ homozygote mutant neonates were born alive but died soon after birth, in the present work, we analyzed adult heterozygote and neonatal mutants. Notably, limb muscles from *Pax3-cre*$^{+/-}$/*Pitx2*$^{+/-}$ heterozygote mice, in which *Pitx2* expression is reduced by >50% (Fig. 8A), displayed higher expression levels of miRNAs regulated by *Pitx2c* (miR-15b, miR-23b, miR-106b, and miR-503) than did *Pax3-cre*$^{+/-}$/*Pitx2*$^{+/+}$ control limb muscles (Fig. 7B). Moreover, given that even in the absence of overt damage, the rate of myonuclear turnover in rodents is 1 to 2% per week (44), we also analyzed the expression levels of the cyclin D1 and cyclin D2 genes, and we found that they were clearly downregulated in

FIG 7 (A) Tissue distribution of miR-15b, miR-23b, miR-106b, and miR-503 in limb muscles of C57BL/10 mice. miRNAs were expressed mostly in cells that presented a tissue distribution very similar to that of satellite cells, as illustrated by Pax7 costaining for miR-106b. An LNA probe with a scrambled sequence was used to test the specificity of the probes. (B) Expression profiles for miR-15b, miR-23b, miR-106b, and miR-503 in *Pax3-cre*$^{+/-}$/*Pitx2*$^{+/-}$ heterozygote mice (n = 9) compared to *Pax3-cre*$^{+/-}$ control mice (n = 8). (C) Cyclin D1 and cyclin D2 gene expression profiles in *Pax3-cre*$^{+/-}$/*Pitx2*$^{+/-}$ heterozygote versus *Pax3-cre*$^{+/-}$ control mice. (D) Expression profiles for miR-15b, miR-23b, miR-106b, and miR-503 in *Pax3-cre*$^{+/-}$/*Pitx2*$^{+/-}$ heterozygote (n = 6) and *Pax3-cre*$^{+/-}$/*Pitx2*$^{-/-}$ homozygote (n = 5) neonates compared to *Pax3-cre*$^{+/-}$ control neonatal mice (n = 6). (E) Cyclin D1 and cyclin D2 gene expression profiles in *Pax3-cre*$^{+/-}$/*Pitx2*$^{+/-}$ heterozygote and *Pax3-cre*$^{+/-}$/*Pitx2*$^{-/-}$ homozygote neonates versus *Pax3-cre*$^{+/-}$ control neonatal mice.

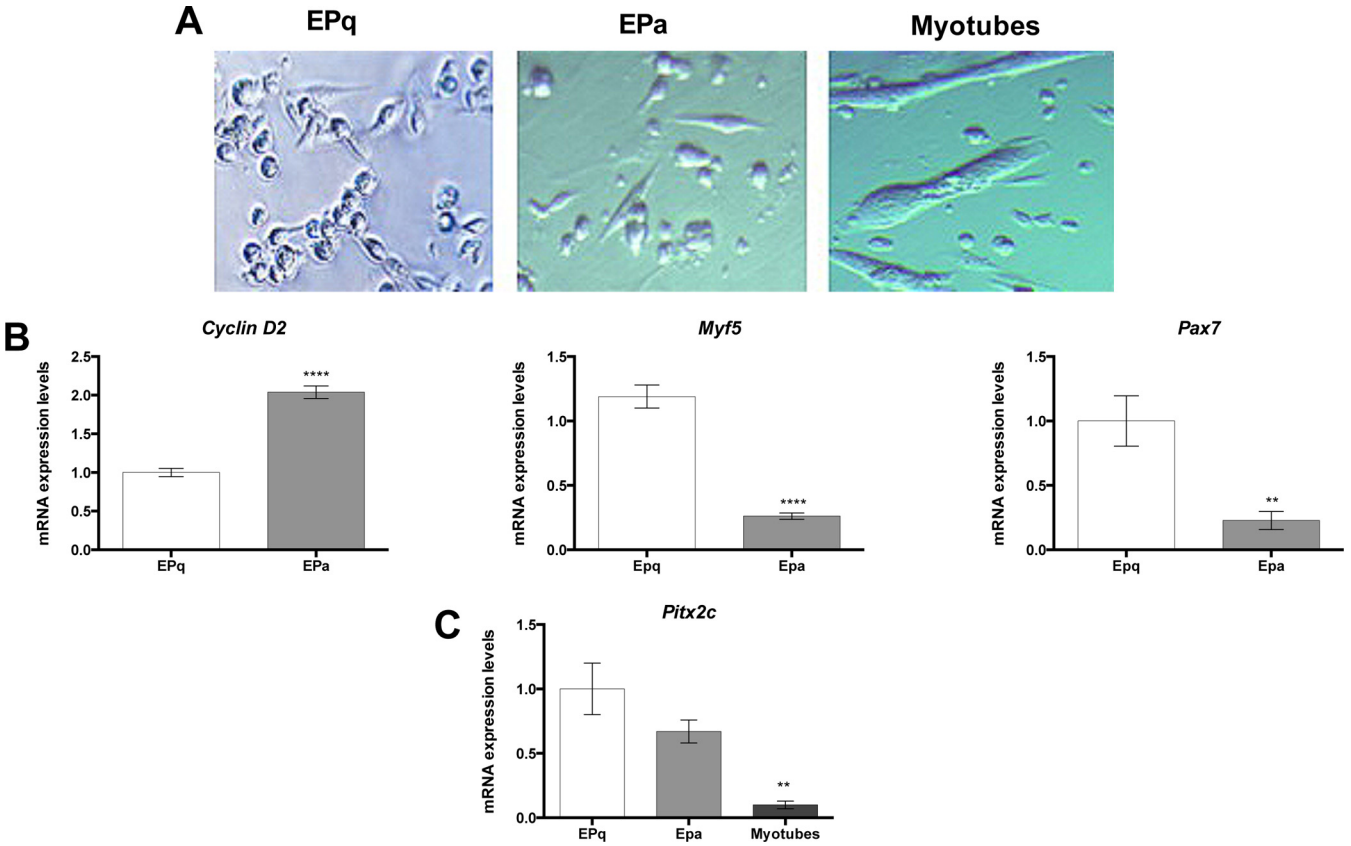

FIG 9 (A) Representative images of early-plated relatively quiescent/early-activated satellite cells (EPq), early-plated long-term-activated satellite cells (EPa), and EPa-derived differentiating fusing-myoblast cultures. (B) mRNA expression levels of the cyclin D2, *Myf5*, and *Pax7* genes in EPq and EPa cells. (C) mRNA expression levels of *Pitx2c* in EPq cells and EPa cells and myoblasts.

Pax3-cre$^{+/-}$*/Pitx2*$^{+/-}$ animals in comparison with control mice (Fig. 7C). These observations are consistent with our *in vitro* findings revealing the existence of a *Pitx2*-miRNA pathway controlling the expression of key regulatory cell cycle genes in myogenic cells. Similar to those from adult mice, limb muscles from *Pax3-cre*$^{+/-}$*/Pitx2*$^{-/-}$ neonatal heterozygote and homozygote mice, which exhibited lower Pitx2c expression levels (Fig. 8B), showed increased levels of miRNAs regulated by *Pitx2c*. Curiously, no changes in cyclin D1 and cyclin D2 gene expression levels were detected in neonatal mutants, pointing out a different status for this *Pitx2*-miRNA pathway in neonates (Fig. 7D and E).

The *Pitx2*-miRNA pathway regulating cell proliferation is conserved in early-activated satellite cells. Given that it was previously shown that Pitx2 can be detected in proliferating myoblasts during adult myogenesis (20), and it appears to help maintain a proliferating pool of myogenic precursor cells in extraocular muscles (45), we next investigated whether the *Pitx2*-miRNA pathway is also present in freshly isolated adult satellite cells. Because adult satellite cells isolated from freshly dissected mouse muscle tissue rapidly initiate the process of activation, leading to myogenic differentiation (36), we first evaluated the expression profile for *Pitx2c* and miRNAs during the *in vitro* process of satellite cell activation and differentiation. Therefore, in the present study, we used early-plated early-activated satellite cells (EPq) and early-plated long-term-activated satellite cells (EPa) isolated from mouse hind limbs according to their adhesion characteristics and proliferation behavior, as previously described (31, 46), as well as EPa-derived differentiating myoblasts fusing to myotubes (Fig. 9A). As illustrated in Fig. 9B, EPq cells can thus be rendered *Pax7* high/low-proliferating cells, and EPa cells can be rendered *Pax7* low-expressing/high-proliferating satellite cells (47). Notably, *Pitx2c* expression levels are higher in early-activated EPq cells than in long-term-activated satellite cells (EPa) and display low expression levels in differentiating myotubes derived from satellite cells (Fig. 9C). This *Pitx2c* expression profile might indicate a Pitx2c requirement just before reaching high levels of cell proliferation during the process of satellite cell activation. Indeed, gain-of-function experiments with EPq and EPa satellite cells showed that *Pitx2c* overexpression leads to a clear upregulation of the cyclin D1 and D2 genes in early-activated satellite cells (EPq) but not in long-term-activated satellite cells (EPa) (Fig. 10A to C). Moreover, the number of Ki67-positive cells was significantly higher in EPq cells overexpressing *Pitx2c* than in cells transfected with the empty lentiviral vector (Fig. 10D and E). These results indicate that *Pitx2c* could regulate proliferation during satellite cell activation.

Next, to test whether *Pitx2c* also acts to control miR-15b, miR-23b, miR-106b, and miR-503 expression in satellite cells, we analyzed miRNA expression profiles on EPq and EPa cells overexpressing *Pitx2c*, and our analyses showed that all miRNAs were dramatically downregulated after *Pitx2c* overexpression (Fig. 11A). Moreover, the miRNAs miR-15b, miR-23b, miR-106b, and

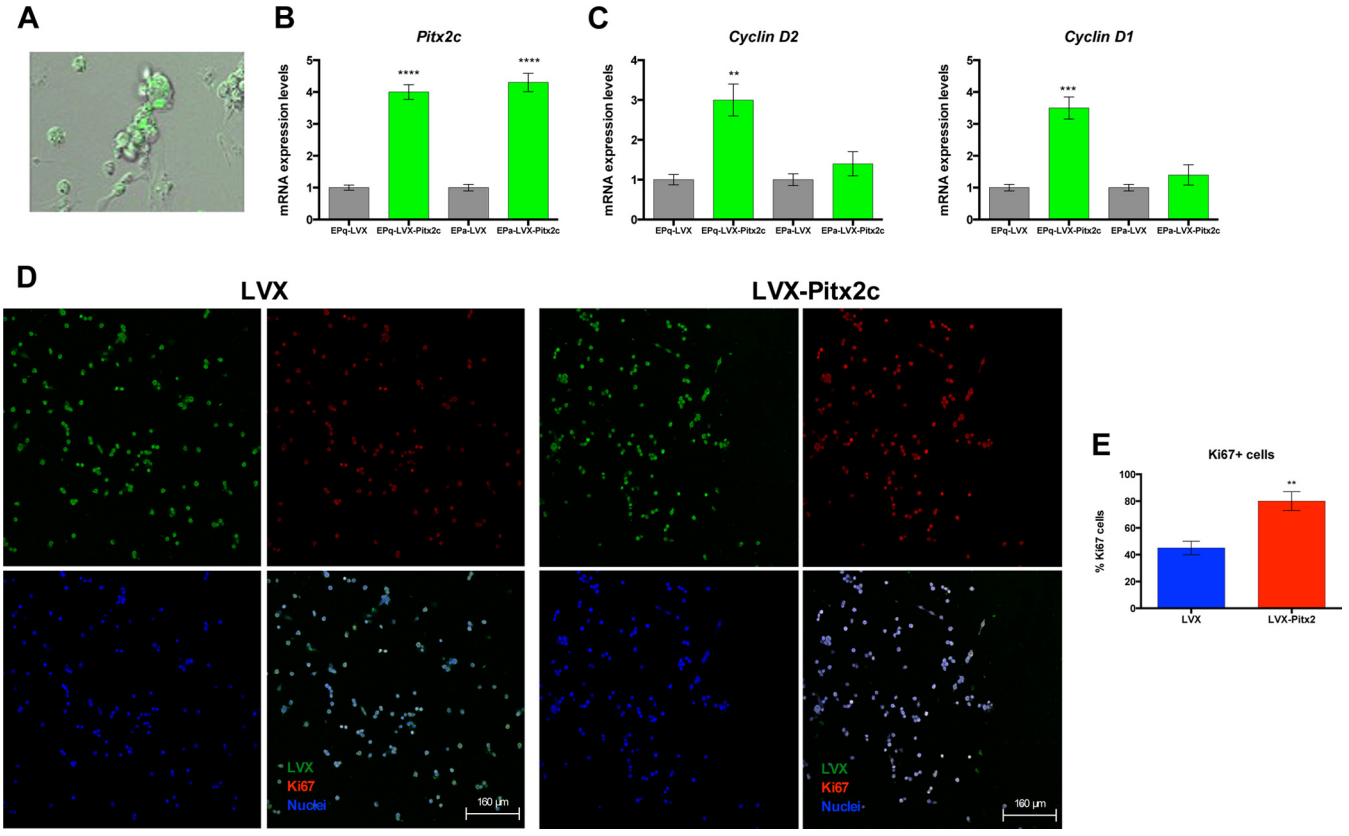

FIG 10 (A) Representative images of EPq cells transfected with a lentivirus-Pitx2c-ZsGreen vector (LVX-Pitx2c). (B) qRT-PCR for *Pitx2c* expression in EPq and EPa cells transfected with the LVX-Pitx2c vector with respect to cells transfected with the empty LVX-ZsGreen lentiviral vector (LVX). (C) Cyclin D1 and cyclin D2 gene expression in EPq and EPa Pitx2c-overexpressing cells with respect to control cells. (D) Representative images of immunohistochemical analyses for Ki67-positve cells in EPq cells transfected with the lentivirus-Pitx2c-ZsGreen vector (LVX) compared to cells transfected with the empty LVX-ZsGreen lentiviral vector (LVX-Pitx2c). (E) Percentage of Ki67$^+$ cells in EPq cells transfected with the lentivirus-Pitx2c-ZsGreen vector with respect to cells transfected with the empty LVX-ZsGreen lentiviral vector.

miR-503 displayed an expression profile complementary to *Pitx2c* during the process of *in vitro* differentiation (Fig. 11B), thus reinforcing the notion that *Pitx2c* acts negatively to regulate these miRNAs in activated satellite cells. The fact that this *Pitx2c*-miRNA pathway is present in EPq and EPa cells but has effects only on cyclin D1 and cyclin D2 gene expression in EPq cells may indicate that the *Pitx2c*-miRNA pathway participates in cell proliferation at an early step of activation but that other regulatory molecules contribute to maintaining cell proliferation after activation is triggered. In accordance with this idea, in neonatal *Pax3-cre*$^{+/-}$/*Pitx2*$^{-/-}$ homozygote mice, altered expression of *Pitx2c*-regulated miRNAs did not lead to cyclin D1 and cyclin D2 gene dysregulation (Fig. 7). Since it was previously shown that many satellite cells at neonatal stages are in a permanent stage of activation to ensure muscle growth (11), these finding emphasize the role of *Pitx2* in cell proliferation at the onset of satellite cell activation but not when the cell activation processes have already taken place. Finally, as observed for Sol8 myoblasts, transfection experiments with a cocktail of these miRNAs in EPq satellite cells resulted in a clear downregulation of the cyclin D1 and cyclin D2 genes (Fig. 11C and D). Moreover, transfection experiments with pre-miR-15b, pre-miR-23b, pre-miR-106b, and pre-miR-503 in *Pitx2c*-overexpressing cells rescued cyclin D1 and cyclin D2 gene upregulation, reinforcing the notion that these miRNAs mediate the *Pitx2c* effects on cyclin D1 and cyclin D2 gene expression (Fig. 12). Therefore, altogether, these findings indicate that the *Pitx2c*-miRNA pathway that modulates cell proliferation is also present in satellite cells.

***Pitx2c* enhances the Myf5$^+$ satellite cell population by regulating miR-106b.** After activation, satellite stem cells expand and undergo symmetric and asymmetric divisions *in vivo* and *in vitro* (48, 49). Symmetric divisions result in the symmetric expansion of Pax7$^+$/Myf5$^-$ satellite cells, retaining their stem cell identity. Through asymmetric divisions, one daughter cell retains its stem cell identity (Pax7$^+$/Myf5$^-$), and the other daughter cell upregulates myogenic factor 5 (Myf5) and becomes Pax7$^+$ Myf5$^+$, representing more committed myogenic progenitors that participate in skeletal-muscle growth and regeneration (36, 49). Myf5 is one of the most relevant transcription factors that plays a key role as a determinant of the acquisition of myogenic cell fate in satellite cells (50, 51). Therefore, in order to test whether *Pitx2c*-mediated effects on cell proliferation can modulate the rate of myogenic commitment of satellite cells, we analyzed *Myf5* expression by qRT-PCR and immunohistochemistry. As illustrated in Fig. 13A, *Myf5* mRNA expression levels were upregulated in *Pitx2c*-overexpressing satellite cells with respect to the control. In addition, the percentage of Myf5$^+$ cells was significantly higher after *Pitx2c* overexpression in satellite cell cultures (Fig. 13B and C). These

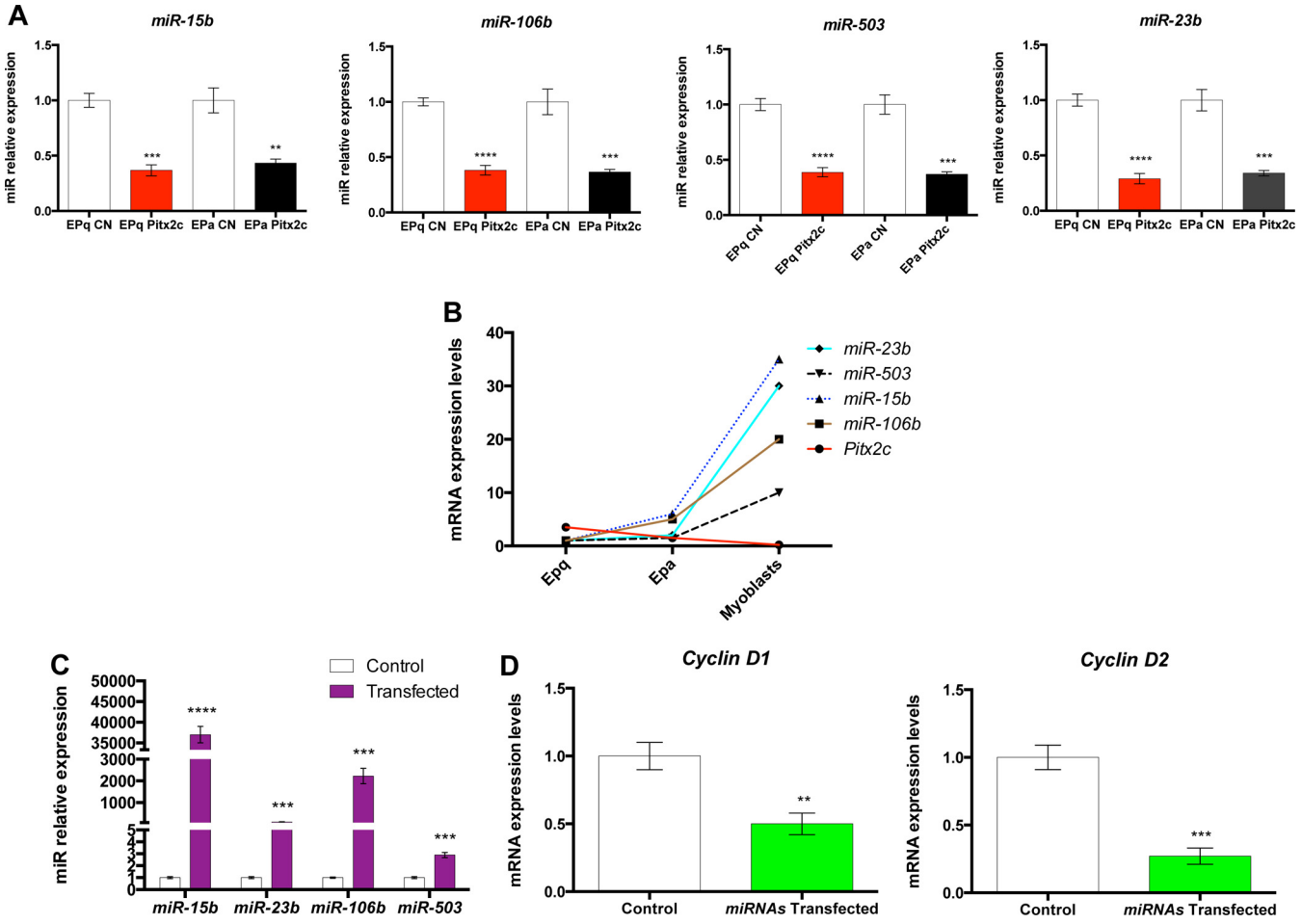

FIG 11 (A) Expression profiles for miR-15b, miR-23b, miR-106b, and miR-503 in EPq and EPa *Pitx2c*-overexpressing cells with respect to control (CN) cells. (B) Relative expression levels of of *Pitx2c* as well as of miR-15b, miR-23b, miR-106b, and miR-503 during myogenic progression. (C and D) miR-15b, miR-23b, miR-106b, and miR-503 overexpression in EPa cells leads to cyclin D1 and cyclin D2 gene downregulation.

results indicate that *Pitx2c* increases the number of Myf5$^+$ satellite cells.

Notably, bioinformatic analyses by TargetScan showed that *Myf5* is a predicted target for the *Pitx2c*-regulated miRNA miR-106b (http://www.targetscan.org/). To validate *Myf5* as a target for miR-106b, we performed pre-miR-106b transfection experiments in satellite cells, and as displayed in Fig. 13D, miR-106b overexpression leads to *Myf5* downregulation. Luciferase reporter assays further validated *Myf5* as a direct target for miR-106b (Fig. 13E). Additionally, pre-miR-106b transfection in *Pitx2c*-overexpressing cells rescued *Myf5* upregulation to basal levels (Fig. 14A to C), supporting the idea that miR-106b is key in mediating the *Pitx2c* effect on *Myf5* gene expression. Thus, since we describe above that miR-106b is a *Pitx2c*-regulated miRNA, we propose that *Pitx2c* enhances *Myf5* expression in satellite cells by regulating miR-106b.

DISCUSSION

Pitx2 is a homeobox transcription factor that has been shown to regulate skeletal-muscle development (15, 16). We previously documented that the c-isoform of *Pitx2* plays a pivotal role in modulating proliferation versus differentiation during myogenesis, balancing the Pax3$^+$/Pax7$^+$ myogenic population *in vivo*, and regulating key myogenic transcription factors such as Pax3 by repressing miR-27b (18, 19). In the present study, we investigated the role of *Pitx2* in controlling microRNA expression in myogenic cells by identifying a subset of *Pitx2c*-regulated miRNAs controlling cell proliferation in myoblasts and demonstrating that this *Pitx2c*-miRNA pathway controls cell proliferation as well as myogenic commitment of satellite cells.

Our analyses revealed that most miRNAs display lower levels after *Pitx2c* overexpression, as revealed by microarray analyses and further validated by qRT-PCR. Importantly, *Pitx2* is sufficient to induce impaired miRNA expression and is also indispensable for regulation of the expression levels of these microRNAs, as revealed by *Pitx2*-silencing experiments. Thus, these data demonstrate the pivotal role of the homeobox transcription factor Pitx2 in controlling microRNA expression in myoblasts. It was recently reported that Pitx2 positively regulates miR-17-92 and miR-106b-25 in the heart (52); however, we found *Pitx2*-mediated negative regulation of miRNA expression in myoblasts. These different functional requirements for Pitx2 underline the differences between cardiac and skeletal myogenesis. Therefore, this study represents the first available description of *Pitx2*-regulated

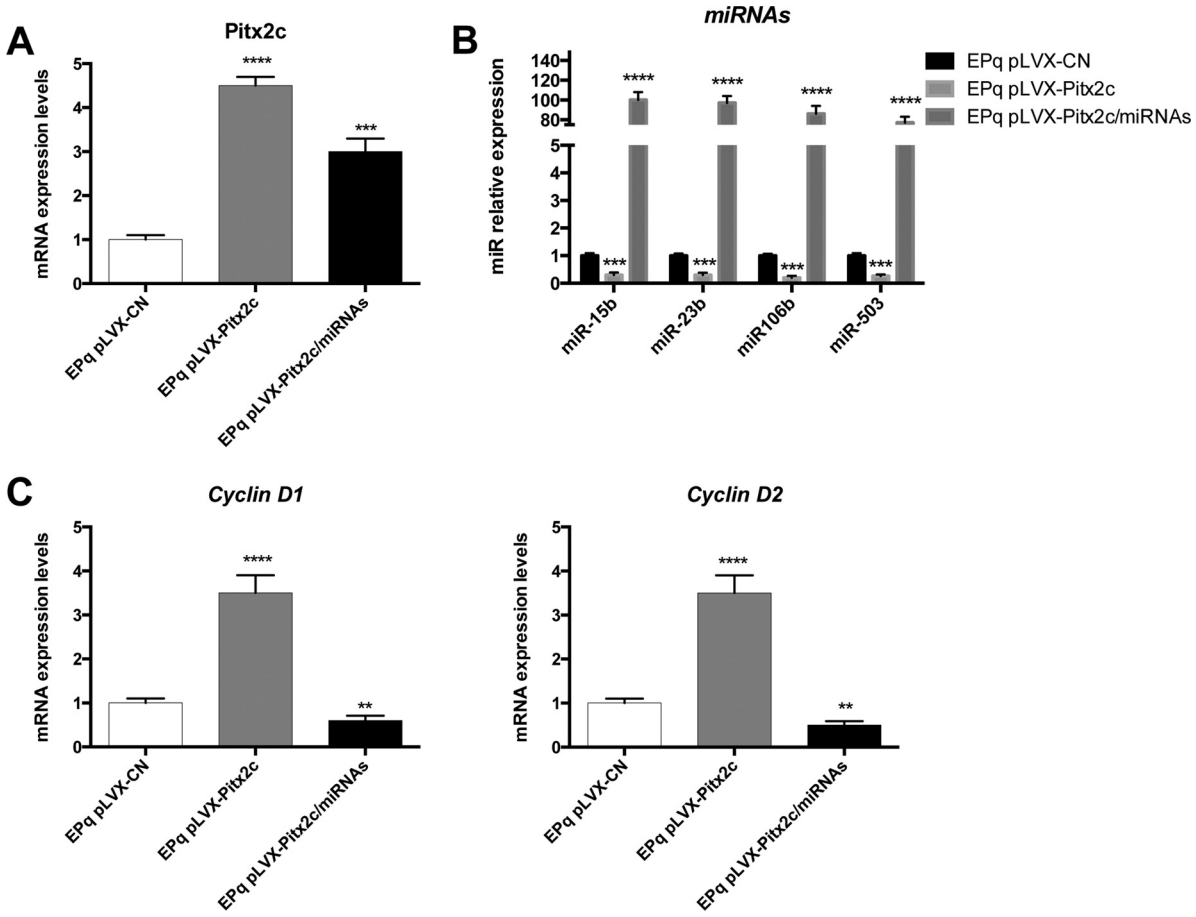

FIG 12 (A) *Pitx2c* overexpression is maintained after pre-miR-106 transfection in EPq cells. (B and C) Pre-miR-106b transfection in EPq cells overexpressing *Pitx2c* (B) rescues cyclin D1 and cyclin D2 gene expression at the basal levels (control cells) (C).

microRNA expression in myogenic cells, providing new insights into the microRNA-mediated mechanisms during myogenesis. Gene ontology analyses have revealed that miRNAs regulated both positively and negatively by *Pitx2c* might lead to modulation of the signaling pathways that control focal adhesion and adherens junction and actin cytoskeleton expression, providing the bases for abnormal cell fusion (18, 19), whereas the miRNAs downregulated by *Pitx2c* also might modulate cell cycle progression in accordance with the previously reported *Pitx2* functions in cell proliferation (18, 19, 45, 53–55). Here, we show that a subset of these *Pitx2c*-downregulated miRNAs, such as miR-15b, miR-106b, miR-23b, and miR-503, targeting cyclins together have dramatic effects on myoblast proliferation *in vitro*, providing a means for the previously reported *Pitx2c* functions in cell proliferation. Furthermore, we show evidence that this *Pitx2*-miRNA pathway that controls cell cycle genes in myogenic cells is also present *in vivo*. Although it has been demonstrated that miR-15b, miR-23b, miR-106b, and miR-503 can regulate the cell cycle (56–59) in different cell types, their functions regarding the regulation of myoblast cell proliferation have not been previously reported.

The role of Pitx2 in satellite cell proliferation and/or differentiation is recently emerging and is controversial. *Pitx2* expression is detected in proliferating satellite cells (20), but the constitutive expression of any *Pitx2* isoform suppresses satellite cell proliferation, with the cells undergoing greater myogenic differentiation (21). Nevertheless, the divergence of the *Pitx2c* effects on satellite cell proliferation found by Knopp et al. (21) could be explained by the moderate *Pitx2c* expression achieved in their *in vitro* gain-of-function experiments, as argued by those authors (21). Even more recently, it was reported that the knockdown of *Pitx2* in satellite cells isolated from extraocular muscles decreased their proliferation rate, and a similar trend was seen for satellite cells isolated from tibialis anterioris muscle (45). Here, we demonstrate that enhanced *Pitx2c* expression boosted cell proliferation in freshly isolated satellite cells, reinforcing the contention that Pitx2 positively regulates cell proliferation in satellite cells.

Notably, we found that the *Pitx2c* expression level was higher in early-activated satellite cells than in long-term-activated satellite cells, and our *in vitro Pitx2c* gain-of-function experiments revealed that *Pitx2c* stimulates cyclin D1 and cyclin D2 gene expression, accelerating cell proliferation during early satellite cell activation. Moreover, we have demonstrated that such *Pitx2c* effects on satellite cell proliferation are mediated by the *Pitx2c*-downregulated miRNAs miR-15b, miR-106b, miR-23b, and miR-503. Recent evidence suggests a role of miRNAs in the regulation of satellite cell fate and self-renewal (27, 29), and it has been reported that miR-106b inhibition augments the number of $Pax7^+$ cells (27). Our findings point out previously unknown functions of miR-15b, miR-106b, miR-23b, and miR-503 in satellite cell proliferation. Since one of the key prerequisites for the triggering

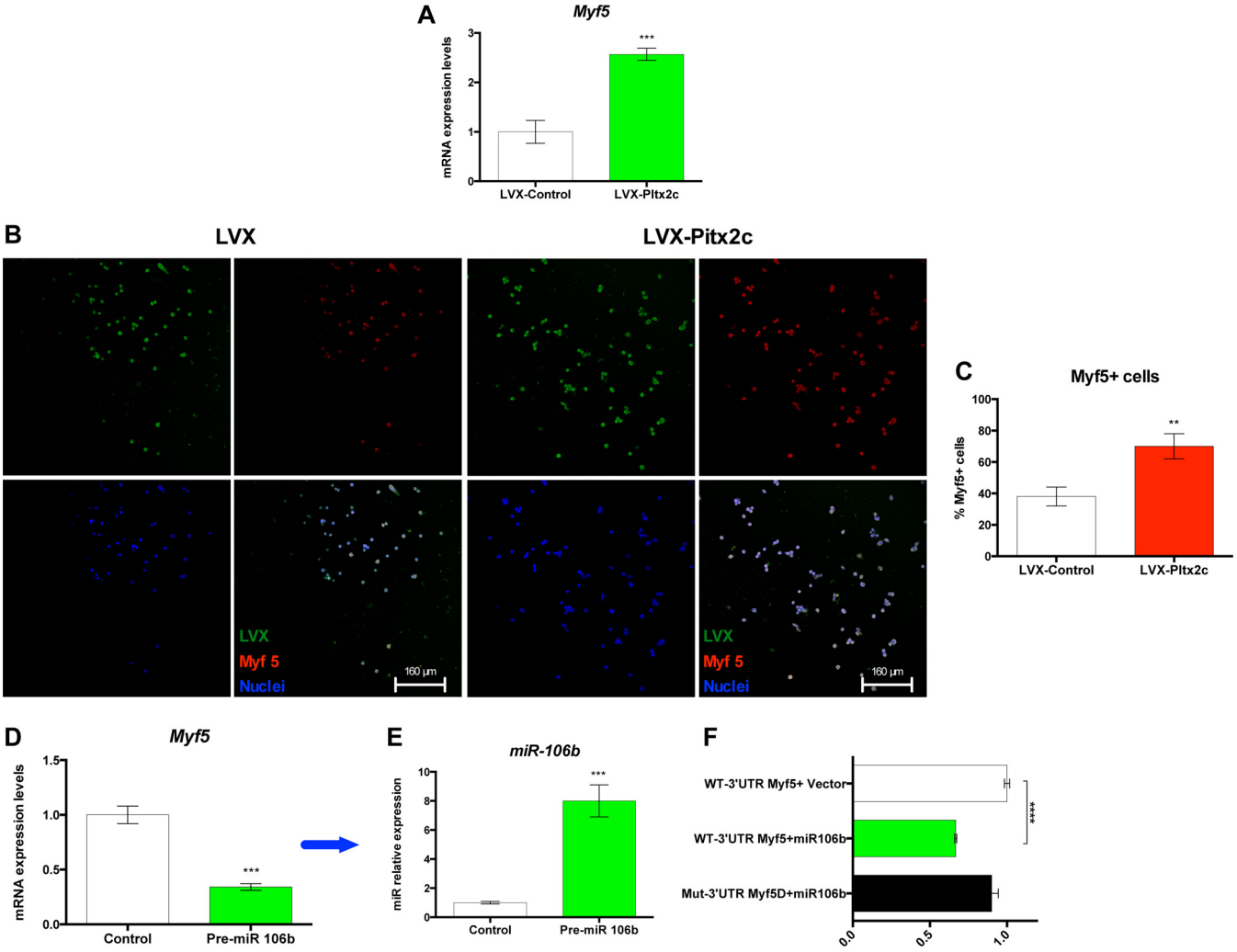

FIG 13 (A) *Myf5* expression profile in EPq *Pitx2c*-overexpressing cells. (B) Representative images of immunohistochemical analyses for Myf5-positive cells in EPq cells transfected with the lentivirus-*Pitx2c*-ZsGreen vector (LVX) compared to cells transfected with the empty LVX-ZsGreen lentiviral vector (LVX-Pitx2c). (C) Percentage of Myf5$^+$ cells in EPq cells transfected with the lentivirus-Pitx2c-ZsGreen vector (LVX-control) with respect to cells transfected with the empty LVX-ZsGreen lentiviral vector (LVX-Pitx2). (D and E) miR-106b overexpression leads to *Myf5* upregulation in EPq cells. (F) Normalized luciferase activity of the 3′-UTR *Myf5* luciferase reporter (wild-type *Myf5* 3′ UTR) with an empty plasmid (vector) or pre-miR-106b shows the loss of luciferase activity with expression of miR-106b. There was no loss of luciferase activity when the miR-106b seed sequence was mutated.

of cell proliferation at the onset of satellite cell activation is proper cell cycle progression (60), the existence of the *Pitx2*-miRNA pathway controlling the expression of key regulatory cell cycle genes in early-activated satellite cells reveals a role of *Pitx2* in satellite cell activation. Although muscle satellite cells are promising targets for cell therapies, the paucity of satellite cells that can be isolated or expanded from adult muscle tissue is limiting; thus, our findings provide new molecular tools to overcome such a bottleneck.

Proliferating satellite cells have a binary fate decision to make: they can differentiate into myoblasts and intercalate into myofibers by fusion to repair the damaged muscle, or they can renew the satellite cell population and return to a quiescent state (36). Quiescent satellite cells expressing paired box 7 (*Pax7*) but with low or undetectable levels of the myogenic regulatory factors Myf5 and MyoD undergo symmetric and asymmetric divisions upon activation. While symmetric expansion of Pax7$^+$/Myf5 satellite stem cells ensures the maintenance of the Pax7$^+$/Myf5$^-$ undifferentiated population, asymmetric divisions generate Pax7$^+$/Myf5$^+$ and Pax7$^+$/Myf5$^-$ daughter cells (36). *Myf5* induction demarcates the entry of satellite stem cells into the myogenic program. Our analyses showed that *Pitx2c* can increase *Myf5* expression by regulating miR-106b, thus enhancing the Myf5$^+$ satellite cell population and revealing a role for *Pitx2c* in promoting satellite cell populations that are more primed for myogenic commitment. The importance of miRNAs in the posttranscriptional regulation of *Myf5* in satellite cells is beginning to emerge. Recently, Crist et al. (61) reported that although many quiescent satellite cells transcribe *Myf5*, they do not enter myogenesis because of miR-31. Thus, miR-31 interacts with the 3′ UTR of *Myf5* mRNA and therefore can prevent its translation into a quiescent cell, but it is rapidly downregulated early during activation, leading to a rapid accumulation of Myf5 protein (61). Here, we demonstrate that downregulation of miR-106b leads to increased *Myf5* expression

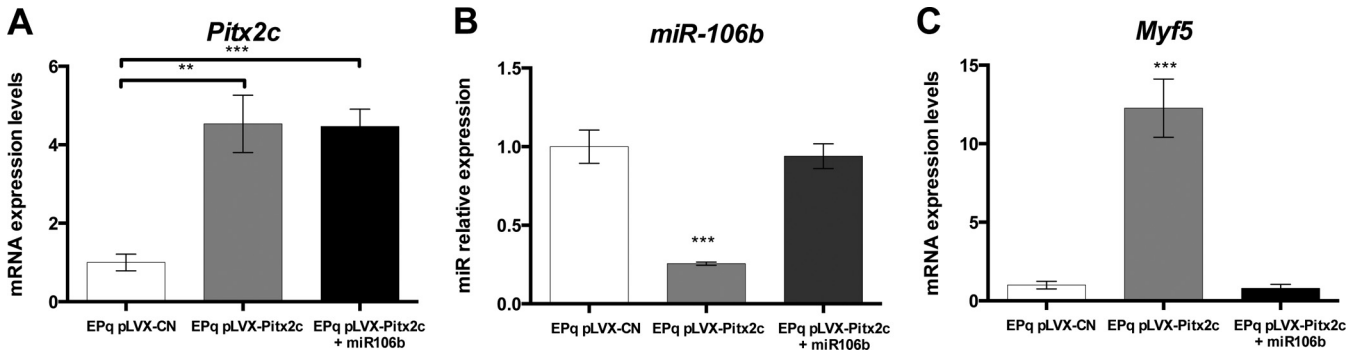

FIG 14 (A) *Pitx2c* overexpression is maintained after pre-miR-106 transfection in EPq cells. (B and C) Pre-miR-106b transfection in EPq cells overexpressing *Pitx2c* (B) rescues *Myf5* expression at basal levels (control cells) (C).

in early-activated satellite cells, thus providing additional information concerning the role of miRNAs in the posttranscriptional control of myogenic progression in adult myogenesis.

On other hand, a mechanism linking *Myf5* levels to muscle stem cell heterogeneity was also recently proposed. A detailed analysis of satellite cell behavior in *Myf5* haploinsufficient mice revealed the duality in the functional role of *Myf5*, as a promoter of muscle fate and also as being incompatible with terminal differentiation, raising questions about the precise role of this transcription factor during different cell states in myogenic lineage progression (50). In the present study, we describe a *Pitx2c*–miR-106b pathway controlling *Myf5* expression, providing new insights into the molecular mechanisms that control satellite cell behavior. These findings might thus have future applications in modulating satellite cell fate during muscle regeneration.

In conclusion, in this paper, we report a subset of microRNAs regulated by *Pitx2*, with previously unknown functions in myogenic cells, which have profound effects on myoblast proliferation. Notably, we found that this *Pitx2*-miRNA pathway regulating cell proliferation is conserved in freshly isolated satellite cells, providing developmental cues that enhance the commitment of satellite cells to myogenic lineage differentiation by downregulating miR-106b expression. Overall, the present study describes a previously unknown *Pitx2*-miRNA pathway controlling cell proliferation in myogenic cells, providing new targets to enhance the regenerative capacity of limb skeletal-muscle myogenic precursor cells for the treatment of skeletal-muscle diseases.

ACKNOWLEDGMENTS

This work was partially supported by grants BFU2012-38111 (Ministerio de Economía y Competitividad, Gobierno de España), CTS-1614, CTS-8053, BIO-302 (Junta de Andalucia), and AFM2012-16074 (AFM).

Estefanía Lozano-Velasco collected and/or assembled data; Daniel Vallejo collected and/or assembled data; Francisco J. Esteban performed data analysis and interpretation; Chris Doherty collected and/or assembled data; Francisco Hernández-Torres collected and/or assembled data; Diego Franco performed data analysis and interpretation and manuscript writing; Amelia Eva Aránega conceived of and designed the study, performed data analysis and interpretation, provided financial support, and performed manuscript writing.

REFERENCES

1. **Chargé SB, Rudnicki MA.** 2004. Cellular and molecular regulation of muscle regeneration. Physiol Rev **84:**209–238. http://dx.doi.org/10.1152/physrev.00019.2003.
2. **Tajbakhsh S, Buckingham M.** 2000. The birth of muscle progenitor cells in the mouse: spatiotemporal considerations. Curr Top Dev Biol **48:**225–268.
3. **Kassar-Duchossoy L, Giacone E, Gayraud-Morel B, Jory A, Gòmes D, Tajbakshs S.** 2005. Pax3/Pax7 mark a novel population of primitive myogenic cells during development. Genes Dev **19:**1426–1431. http://dx.doi.org/10.1101/gad.345505.
4. **Relaix F, Rocancourt D, Mansouri A, Buckingham M.** 2005. A Pax3/Pax7-dependent population of skeletal muscle progenitor cells. Nature **435:**948–953. http://dx.doi.org/10.1038/nature03594.
5. **Bajard L, Relaix F, Rocancourt D, Daubas P, Buckingham ME.** 2006. A novel genetic hierarchy functions during hypaxial myogenesis: Pax3 directly activates Myf5 in muscle progenitor cells in the limb. Genes Dev **20:**2450–2464. http://dx.doi.org/10.1101/gad.382806.
6. **Buckingham ME, Relaix F.** 2007. The role of Pax genes in the development of tissues and organs: Pax3 and Pax7 regulate muscle progenitor cell functions. Annu Rev Cell Dev Biol **23:**645–673. http://dx.doi.org/10.1146/annurev.cellbio.23.090506.123438.
7. **Hu P, Geles KG, Paik JH, DePinho RA, Tjian R.** 2008. Codependent activators direct myoblast-specific MyoD transcription. Dev Cell **15:**534–546. http://dx.doi.org/10.1016/j.devcel.2008.08.018.
8. **McKinnell LW, Ishibashi J, Le Grand F, Punch VG, Addicks GC, Greenblatt JF, Dilworth FJ, Rudnicki MA.** 2008. Pax7 activates myogenic genes by recruitment of a histone methyltransferase complex. Nat Cell Biol **10:**77–84. http://dx.doi.org/10.1038/ncb1671.
9. **Horst D, Ustanina S, Sergi C, Mikuz G, Juergens H, Braun T, Vorobyov E.** 2006. Comparative expression analysis of Pax3 and Pax7 during mouse myogenesis. Int J Dev Biol **50:**47–54. http://dx.doi.org/10.1387/ijdb.052111dh.
10. **Montarras D, Morgan J, Collins C, Relaix F, Zaffran S, Cumano A, Partridge T, Buckingham M.** 2005. Direct isolation of satellite cells for skeletal muscle regeneration. Science **309:**2064–2067. http://dx.doi.org/10.1126/science.1114758.
11. **Relaix F, Montarras D, Zaffran S, Gayraud-Morel D, Rocancourt D, Tajbakhsh S, Mansouri A, Cumano A, Buckingham M.** 2006. Pax3 and Pax7 have distinct and overlapping functions in adult muscle progenitors cells. J Cell Biol **172:**91–102. http://dx.doi.org/10.1083/jcb.200508044.
12. **Zammit PS, Cohen A, Buckingham ME, Kelly RG.** 2008. Integration of embryonic and fetal skeletal myogenic programs at the myosin light chain 1f/3f locus. Dev Biol **313:**420–433. http://dx.doi.org/10.1016/j.ydbio.2007.10.044.
13. **Collins CA, Olsen I, Zammit PS, Heslop L, Petrie A, Partridge TA, Morgan JE.** 2005. Stem cell function, self-renewal, and behavioral heterogeneity of cells from the adult muscle satellite niche. Cell **122:**289–301. http://dx.doi.org/10.1016/j.cell.2005.05.010.
14. **L'Honoré A, Coulon V, Marcil A, Lebel M, Lafrance-Vanasse J, Gage P, Camper S, Drouin J.** 2007. Sequential expression and redundancy of Pitx2 and Pitx3 genes during muscle development. Dev Biol **307:**421–433. http://dx.doi.org/10.1016/j.ydbio.2007.04.034.
15. **Zacharias AL, Lewandoski M, Rudnicki MA, Gage PJ.** 2011. Pitx2 is an upstream activator of extraocular myogenesis and survival. Dev Biol **349:**395–405. http://dx.doi.org/10.1016/j.ydbio.2010.10.028.
16. **L'Honoré A, Ouimette JF, Lavertu-Jolin M, Drouin J.** 2010. Pitx2 defines alternate pathways acting through MyoD during limb and somatic

myogenesis. Development **137:**3847–3856. http://dx.doi.org/10.1242/dev.053421.
17. **L'Honoré A, Commère PH, Ouimette JF, Montarras D, Drouin J, Buckingham M.** 2014. Redox regulation by Pitx2 and Pitx3 is critical for fetal myogenesis. Dev Cell **29:**392–405. http://dx.doi.org/10.1016/j.devcel.2014.04.006.
18. **Martínez-Fernández S, Hernández-Torres F, Franco D, Lyons GE, Navarro F, Aránega AE.** 2006. Pitx2c overexpression promotes cell proliferation and arrests differentiation in myoblasts. Dev Dyn **235:**2930–2939. http://dx.doi.org/10.1002/dvdy.20924.
19. **Lozano-Velasco E, Contreras A, Crist C, Franco D, Aránega AE.** 2011. Pitx2c modulates Pax3+/Pax7+ cell populations and regulates Pax3 expression by repressing miR27 expression during myogenesis. Dev Biol **357:**165–178. http://dx.doi.org/10.1016/j.ydbio.2011.06.039.
20. **Ono Y, Boldrin L, Knopp P, Morgan JE, Zammit PS.** 2010. Muscle satellite cells are a functionally heterogeneous population in both somite-derived and branchiomeric muscles. Dev Biol **337:**29–41. http://dx.doi.org/10.1016/j.ydbio.2009.10.005.
21. **Knopp P, Figeac N, Fortier M, Moyle L, Zammit PS.** 2013. Pitx genes are replayed in adult myogenesis where they can act to promote myogenic differentiation in muscle satellite cells. Dev Biol **377:**293–304. http://dx.doi.org/10.1016/j.ydbio.2013.02.011.
22. **Chen JF, Tao Y, Li J, Deng Z, Yan Z, Xiao X, Wang DZ.** 2010. MicroRNA-1 and microRNA-206 regulate skeletal muscle satellite cell proliferation and differentiation by repressing Pax7. J Cell Biol **190:**867–879. http://dx.doi.org/10.1083/jcb.200911036.
23. **Huang MB, Xu H, Xie SJ, Zhou H, Qu LH.** 2011. Insulin-like growth factor-1 receptor is regulated by microRNA-133 during skeletal myogenesis. PLoS One **6:**e29173. http://dx.doi.org/10.1371/journal.pone.0029173.
24. **Dey BK, Gagan J, Dutta A.** 2011. miR-206 and -486 induce myoblast differentiation by downregulating Pax7. Mol Cell Biol **31:**203–214. http://dx.doi.org/10.1128/MCB.01009-10.
25. **Gagan J, Dey BK, Layer R, Yan Z, Dutta A.** 2011. MicroRNA-378 targets the myogenic repressor MyoR during myoblast differentiation. J Biol Chem **286:**19431–19438. http://dx.doi.org/10.1074/jbc.M111.219006.
26. **Crist CG, Montarras D, Pallafacchina G, Rocancourt D, Cumano A, Conway SJ, Buckingham M.** 2009. Muscle stem cell behavior is modified by microRNA-27 regulation of Pax3 expression. Proc Natl Acad Sci U S A **106:**13383–13387. http://dx.doi.org/10.1073/pnas.0900210106.
27. **Farina NH, Hausburg M, Betta ND, Pulliam C, Srivastava D, Cornelison D, Olwin BB.** 2012. A role for RNA post-transcriptional regulation in satellite cell activation. Skelet Muscle **2:**21. http://dx.doi.org/10.1186/2044-5040-2-21.
28. **Cheung TH, Quach NL, Charville GW, Liu L, Park L, Edalati A, Yoo B, Hoang P, Rando TA.** 2012. Maintenance of muscle stem-cell quiescence by microRNA-489. Nature **482:**524–528. http://dx.doi.org/10.1038/nature10834.
29. **Koning M, Werker PM, van Luyn MJ, Krenning G, Harmsen MC.** 2012. A global downregulation of microRNAs occurs in human quiescent satellite cells during myogenesis. Differentiation **84:**314–321. http://dx.doi.org/10.1016/j.diff.2012.08.002.
30. **Tessari AM, Pietrobon A, Notte A, Cifelli G, Gage PJ, Schneider MD, Lembo G, Campione M.** 2008. Myocardial Pitx2 differentially regulates the left atrial identity and ventricular asymmetric remodelling programs. Circ Res **102:**813–822. http://dx.doi.org/10.1161/CIRCRESAHA.107.163188.
31. **Qu-Petersen Z, Deasy B, Jankowski R, Ikezawa M, Cummins J, Pruchnic R, Mytinger J, Cao B, Gates C, Wermig A, Huard J.** 2002. Identification of a novel population of muscle stem cells in mice: potential for muscle regeneration. J Cell Biol **157:**851–864. http://dx.doi.org/10.1083/jcb.200108150.
32. **Richler C, Yaffe D.** 1970. The in vitro cultivation and differentiation capacities of myogenic cell lines. Dev Biol **23:**1–22. http://dx.doi.org/10.1016/S0012-1606(70)80004-5.
33. **Rando TA, Blau HM.** 1994. Primary mouse myoblast purification, characterization, and transplantation for cell-mediated gene therapy. J Cell Biol **125:**1275–1287. http://dx.doi.org/10.1083/jcb.125.6.1275.
34. **Qu Z, Balkir L, van Deutekom JCT, Robbins PD, Pruchnic R, Huard J.** 1998. Development of approaches to improve cell survival in myoblast transfer therapy. J Cell Biol **142:**1257–1267. http://dx.doi.org/10.1083/jcb.142.5.1257.
35. **Qu Z, Huard J.** 2000. Matching host muscle and donor myoblast for myosin heavy chain improves myoblast transfer therapy. Gene Ther **7:**428–437. http://dx.doi.org/10.1038/sj.gt.3301103.
36. **Yin H, Price F, Rudnicki MA.** 2013. Satellite cells and the muscle stem cell niche. Physiol Rev **93:**23–67. http://dx.doi.org/10.1152/physrev.00043.2011.
37. **Livak KJ, Schmittgen TD.** 2001. Analysis of relative gene expression data using real-time quantitative PCR and the 2(-Delta Delta C(T)) method. Methods **25:**402–408. http://dx.doi.org/10.1006/meth.2001.1262.
38. **Domínguez JN, Navarro F, Franco D, Thompson RP, Aránega AE.** 2005. Temporal and spatial expression pattern of beta1 sodium channel subunit during heart development. Cardiovasc Res **65:**842–850. http://dx.doi.org/10.1016/j.cardiores.2004.11.028.
39. **Goljanek-Whysall K, Sweetman D, Abu-Elmagd M, Chapnik E, Dalmay T, Hornstein E, Münsterberg A.** 2011. MicroRNA regulation of the paired-box transcription factor Pax3 confers robustness to developmental timing of myogenesis. Proc Natl Acad Sci U S A **108:**11936–11941. http://dx.doi.org/10.1073/pnas.1105362108.
40. **Nielsen BS, Holmstrom K.** 2013. Combined microRNA in situ hybridization and immunohistochemical detection of protein markers. Methods Mol Biol **986:**353–365. http://dx.doi.org/10.1007/978-1-62703-311-4_22.
41. **Cao H, Jheon A, Li X, Wang J, Florez S, Zhang Z, McManus MT, Klein OD, Amendt BA.** 2013. The Pitx2:miR-200c/141:noggin pathway regulates Bmp signaling and ameloblast differentiation. Development **140:**3348–3359. http://dx.doi.org/10.1242/dev.089193.
42. **Edgar R, Domrachev M, Lash AE.** 2002. Gene Expression Omnibus: NCBI gene expression and hybridization array data repository. Nucleic Acids Res **30:**207–210. http://dx.doi.org/10.1093/nar/30.1.207.
43. **Abu-Elmagd M, Robson L, Sweetman D, Hadley J, Francis-West P, Münsterberg A.** 2010. Wnt/Lef1 signaling acts via Pitx2 to regulate somite myogenesis. Dev Biol **337:**211–219. http://dx.doi.org/10.1016/j.ydbio.2009.10.023.
44. **Schmalbruch H, Lewis DM.** 2000. Dynamics of nuclei of muscle fibers and connective tissue cells in normal and denervated rat muscles. Muscle Nerve **23:**617–626. http://dx.doi.org/10.1002/(SICI)1097-4598(200004)23:4<617::AID-MUS22>3.0.CO;2-Y.
45. **Hebert SL, Daniel ML, McLoon NK.** 2013. The role of Pitx2 in maintaining the phenotype of myogenic precursor cells in the extraocular muscles. PLoS One **8:**e58405. http://dx.doi.org/10.1371/journal.pone.0058405.
46. **Lavasani M, Lu A, Thompson SD, Robbins PD, Huard J, Neidernhofer LJ.** 2013. Isolation of muscle-derived stem/progenitor cells based on adhesion characteristics to collagen-coated surfaces. Methods Mol Biol **976:**53–65. http://dx.doi.org/10.1007/978-1-62703-317-6_5.
47. **Rocheteau P, Gayraud-Morel B, Siegl-Cachedenier L, Blasco MA, Tajbakhsh S.** 2012. A subpopulation of adult skeletal muscle stem cells retains all template DNA strands after cell division. Cell **148:**112–125. http://dx.doi.org/10.1016/j.cell.2011.11.049.
48. **Shinin V, Gayraud-Morel D, Gomès D, Tajbakhsh S.** 2006. Asymmetric division and cosegregation of template DNA strands in adult muscle satellite cells. Nat Cell Biol **8:**677–687. http://dx.doi.org/10.1038/ncb1425.
49. **Wang YX, Rudnicki MA.** 2011. Satellite cells, the engines of muscle repair. Nat Rev Mol Cell Biol **13:**127–133. http://dx.doi.org/10.1038/nrm3265.
50. **Kassar-Duchossoy L, Gayraud-Morel B, Gomès D, Rocancourt D, Buckingham M, Shinin V, Tajbakhsh S.** 2004. Mrf4 determines skeletal muscle identity in Myf5:Myod double-mutant mice. Nature **431:**466–471. http://dx.doi.org/10.1038/nature02876.
51. **Gayraud-Morel B, Chrètien F, Jory A, Sambasivan R, Negroni E, Flamant P, Soubigou G, Coppée JY, Di Santo J, Cumano A, Mouly V, Tajbakhsh S.** 2012. Myf5 haploinsufficiency reveals distinct cell fate potentials for adult skeletal muscle stem cells. J Cell Sci **125**(Part 7):1738–1749. http://dx.doi.org/10.1242/jcs.097006.
52. **Wang J, Bai Y, Li N, Ye W, Zhang M, Greene SB, Tao Y, Chen Y, Wehrens XH, Martin JF.** 2014. Pitx2-microRNA pathway that delimits sinoatrial node development and inhibits predisposition to atrial fibrillation. Proc Natl Acad Sci U S A **111:**9181–9186. http://dx.doi.org/10.1073/pnas.1405411111.
53. **Kioussi C, Briata P, Baek SH, Rose DW, Hamblet NS, Herman T, Ohgi KA, Lin C, Gleiberman A, Wang J, Brault V, Ruiz-Lozano P, Nguyen HD, Kémler R, Glass CK, Wynshaw-Boris A, Rosenfeld MG.** 2002. Identification of a Wnt/Dvl/beta-catenin → Pitx2 pathway mediating cell-type-specific proliferation during development. Cell **111:**673–685. http://dx.doi.org/10.1016/S0092-8674(02)01084-X.

54. **Gherzi R, Trabucchi M, Ponassi M, Gallouzi IE, Rosenfeld MG, Briata P.** 2010. Akt2-mediated phosphorylation of Pitx2 controls Ccnd1 mRNA decay during muscle cell differentiation. Cell Death Differ **17:**975–983. http://dx.doi.org/10.1038/cdd.2009.194.
55. **Huang Y, Guigon CJ, Fan J, Cheng SY, Zhu GZ.** 2010. Pituitary homeobox 2 (PITX2) promotes thyroid carcinogenesis by activation of cyclin D2. Cell Cycle **9:**1333–1341. http://dx.doi.org/10.4161/cc.9.7.11126.
56. **Kim S, Kang H.** 2013. miR-15b induced by platelet-derived growth factor signaling is required for vascular smooth muscle cell proliferation. BMB Rep **46:**550–554. http://dx.doi.org/10.5483/BMBRep.2013.46.11.057.
57. **Tian L, Fang YX, Xue JL, Chen JZ.** 2013. Four microRNAs promote prostate cell proliferation with regulation of PTEN and its downstream signals in vitro. PLoS One **8:**e75885. http://dx.doi.org/10.1371/journal.pone.0075885.
58. **Yao YL, Wu XY, Wu JH, Gu T, Chen L, Gu JH, Liu Y, Zhang QH.** 2013. Effects of microRNA-106 on proliferation of gastric cancer cell through regulating p21 and E2F5. Asian Pac J Cancer Prev **14:**2839–2843. http://dx.doi.org/10.7314/APJCP.2013.14.5.2839.
59. **Xiao F, Zhang W, Chen L, Chen F, Xie H, Xing C, Yu X, Ding S, Chen K, Guo H, Cheng J, Zheng S, Zhou L.** 2013. MicroRNA-503 inhibits the G1/S transition by downregulating cyclin D3 and E2F3 in hepatocellular carcinoma. J Transl Med **11:**195. http://dx.doi.org/10.1186/1479-5876-11-195.
60. **De Luca G, Ferretti R, Brschi M, Mezaroma E, Caruso M.** 2013. Cyclin d3 critically regulates the balance between self-renewal and differentiation in skeletal muscle stem cells. Stem Cells **31:**2478–2491. http://dx.doi.org/10.1002/stem.1487.
61. **Crist CG, Montarras D, Bckingham M.** 2012. Muscle satellite cells are primed for myogenesis but maintain quiescence with sequestration of Myf5 mRNA targeted by microRNA-31 in mRNP granules. Cell Stem Cell **11:**118–126. http://dx.doi.org/10.1016/j.stem.2012.03.011.